Lawrence Berkeley National Laboratory
Recent Work

Title

PHYSICS DIVISION QUARTERLY REPORT, NOV., DEC. 1950 AND JAN. 1951

Permalink

https://escholarship.org/uc/item/98z84737

Author

Lawrence Berkeley National Laboratory

Publication Date

1951-03-20

UNIVERSITY OF CALIFORNIA – BERKELEY

RADIATION LABORATORY

DISCLAIMER

UNIVERSITY OF CALIFORNIA
Radiation Laboratory

Cover Sheet
Do not remove

INDEX NO. _UCRL 1191_
This document contains _____ pages
This is copy _3_, of _____ series ___

Issued to _Inf Div_.

Each person who receives this document must sign the cover sheet in the space below.

Route to	Noted by	Date	Route to	Noted by	Date
L Henrich	LRHff	7-29-52			
WQK					
M Smith	✓				

5(M)

UNIVERSITY OF CALIFORNIA

Radiation Laboratory

Contract No. W-7405-eng-48

UNCLASSIFIED

PHYSICS DIVISION QUARTERLY REPORT

November, December, 1950 and January, 1951

March 20, 1951

Some of the results reported in this document may be
of a preliminary or incomplete nature. It is the
request of the Radiation Laboratory that the document
not be circulated off the project nor the results
quoted without permission.

Berkeley, California

TABLE OF CONTENTS

-3-

I GENERAL PHYSICS RESEARCH

1. Cloud Chamber Program
Scattering of High Energy Deuterons by 90 Mev Neutrons

Wilson M. Powell

Introduction. The scattering by deuterons of protons and neutrons of energies below 14 Mev has been studied experimentally by several groups[1-7] and theoreti- cally by Buckingham and Massey[8,9], and the agreement between experiment and theory has thrown some light on the behavior of deuterons bombarded by neutrons in this energy range. The inherent difficulty of the problem simplifies in some respects if the energies become higher as shown by the theoretical work of Geoffrey F. Chew[10,11]. The simplest guess would be that with 90 Mev neutrons the binding energy of the deuteron would be negligible and the scattering could be considered as the sum of that due to a proton and an independent neutron. As might be expected, Chew points out that this oversimplifies the problem and does not show the large elastic cross section which is predicted theoreti- cally and is found to exist experimentally. The production of fast deuterons among the reaction products from nuclear bombardments by 90 Mev neutrons was observed experimentally by York[12,13] with proportional counters and by Brueckner and Powell[14] in a cloud chamber, and the deuterons were found to have energies of the order of 90 Mev, indicating that there is a much larger probability of of the deuteron surviving an energetic collision than would be expected. Chew's discussions of this problem show that for neutron-deuteron collisions of 90 Mev the elastic cross section is quite large and arises from the fact that the incoming neutron can remove the proton from a deuteron when the proton in the deuteron has a momentum and position which is consistent with the formation of a new deuteron with the incoming neutron. The incoming neutron robs the deuteron of its proton and escapes with it. This interesting process results in a large cross section for deuterons scattered in a forward direction. Another group of collisions will occur where the neutron removes the neutron from the stationary deuteron so rapidly that the remaining proton is left be- hind with a more or less isotropic momentum distribution. As a consequence of this a group of protons of low energy should be and are observed going backwards at angles of more than 90° to the neutron beam. The results given in this experiment illustrate the various points made in Chew's theory very well, and the quantitative agreement between theory and experiment is excellent.

Apparatus. 1. The Cloud Chamber. The 90 Mev neutrons produced in the strip- ping process[15] by bombarding a half-inch beryllium target with 190 Mev deuterons were collimated by means of a rectangular copper collimator four feet long giving a beam 2-3/4 inches wide and 3/4 inch high before entering a 3 x 1 inch, five mil thick, copper window in a large 22 inch diameter Wilson cloud chamber[16] placed outside the concrete shielding around the 184-inch cyclotron. The neu- trons passed through the center of the chamber and through a second window similar to the first so as to reduce the back-scattering of neutrons in the rear wall of the chamber. Deuterium gas at 100 cm pressure with heavy water vapor

was used for filling the chamber so that only deuterium and oxygen appeared. The movable plate forming the bottom of the active part of the cloud chamber consists of a rubber covered, half-inch thick lucite disk which moves vertically, controlled by a pantagraph which keeps it accurately horizontal during the expansion of the chamber. This plate was covered with gelatin dissolved in heavy water which contained a black dye so that it made a very black background. So little light was scattered by this surface that the lights could be directed on it and tracks could still be seen. The 3-1/2 inch high chamber had uniform illumination over 2-1/2 inches.

2. The Light Source. Great care was taken to make the illumination uniform. Each light consisted of a General Electric FT422 flash tube wrapped in aluminum foil which covered the back half of the tube. The foil was held on by winding a 5-mil wolfram wire in a spiral with a half-inch spacing around the tube; this wire and the aluminum foil acted as the tickler electrode. Five 4-1/2 inch diameter double convex lenses of 6 inch focal length were ground down a quarter of an inch at adjacent edges so that they could be placed with axes 4 inches apart. These were located about 6-1/2 inches from the flash tube, and cardboard baffles covered with black velvet passed between the lenses back to the flash tube so that each lens saw only 4 inches of flash tube. The beam of light was quite uniform over 2.5 inches in a vertical direction at the center of the cloud chamber. This was tested by exposing Ozalid printing paper to about 25 flashes of the light. This high contrast paper indicated that the light was uniform probably to better than 20 percent over this vertical height. Without correction the illumination at the center of the chamber was about twice as great as at the edge if it was measured along a horizontal line parallel to the light source. In order to correct this, narrow strips of black scotch tape were placed across the lights at intervals until a photoelectric measurement of the intensity of the light showed that there were no variations greater than 10 percent. With this uniform illumination it was possible to obtain excellent pictures using an f number of 8 and Eastman Linagraph Orthocromatic film.

3. The Magnet. The cloud chamber is operated in a magnetic field of 22,000 gauss which is turned on in advance, reaching its maximum in 2.5 seconds when the chamber is expanded, the cyclotron pulsed, and the lights flashed. The magnet is turned off immediately after the arrival of the beam. A picture is taken once a minute. The magnetic field varies by as much as 6 percent over the region where tracks were measured, but this was corrected for by determining the field at all points of the chamber and using the strength of the field at the center of the measured part of each track. Second order corrections for variation of the magnetic field along the track were negligible.

The Neutron Beam. The neutron beam has a considerable energy spread[17,18] with a maximum at about 90 Mev and a half width of between 25 and 30 Mev. It was collimated after emerging from the three inch diameter hole in the concrete shielding by means of a four foot long copper collimator with a 2-3/4 x 3/4 inch opening as mentioned above and shown in Fig. 1. A few low energy deuterons going backwards and starting in the gas of the chamber gave evidence that there were a few low energy neutrons not travelling parallel to the main beam, but these disappeared when the second thin window at the rear of the chamber was installed. Apparently these neutrons were produced in the rear wall of the

chamber and their presence for a few of the earliest pictures do not affect the results of the experiment. Approximately ten events appeared in the gas of the chamber outside of the beam of neutrons. These were in most cases slow deuterons, and their small number indicates that no appreciable error can arise from neglecting their presence.

Fig. 2 is a histogram of the number of elastically scattered deuterons produced by neutrons in ten Mev intervals and it shows a peak around 80 Mev and another peak at 5 Mev with a valley extending from 45 Mev to 10 Mev. The 80 Mev peak is lower than expected by about 5 Mev but the lack of any correction for a cross section probably accounts fully for this shift. The peak at 5 Mev becomes very small if the cross section is assumed to be inversely proportional to the neutron energy, and it is similar to one observed with hydrogen in the chamber[18].

Identification of Protons and Deuterons. The method used for distinguishing protons and deuterons at high energies rests on the determination of magnetic rigidity $B\rho$ and specific ionization. No success could be expected were it not for the fact that only protons and deuterons could start in the gas of the chamber, and therefore it was necessary only to distinguish between the specific ionization for these two particles. A deuteron with the same $B\rho$ as a proton was approximately three times the specific ionization. A deuteron with the same ionization as a proton has twice the radius of curvature, and it is possible with care in the technique to distinguish between the two in all cases. At low energies range and $B\rho$ are used or the change in $B\rho$ along the track. At very high energies the maximum value for the $B\rho$ of a proton is less than that which can appear in a deuteron because there are no neutrons with energies above 135 Mev and probably none with energies above 125 Mev. This means that the most energetic deuterons have a $B\rho$ which makes them unmistakable and any particle appearing with less specific ionization than one of these deuterons must be a proton.

Fig. 3 shows a proton, 1, colliding with a deuteron, 2, in the gas of the chamber and recoiling backwards, 3. The incoming proton is finely ionizing and curved more than the more heavily ionizing deuteron and the identification is unambiguous. The momentum balance is an additional check in this case. The contrast of the Eastman Orthochromatic Linagraph film is quite great and considerable care was taken to use it at such an exposure that the difference in specific ionization would show. The chamber was operated with quite a background of fine droplets which do not show in the pictures because the exposure is not intense enough to make individual droplets appear on the negative. Clusters of droplets, however, produce a dark image on the negative. To increase the contrast, the film was developed for 14 minutes in Eastman D-19 developer at 68° Fahrenheit and with constant agitation. The film is raised and lowered in the developer continuously, and this results in much better contrast. All of these precautions plus the accurate setting of the lights result in there being no cases where two observers were unable to agree on the identity of the particle observed. Fig. 4 shows examples of both deuterons and protons. The horizontal lines are clearing field wires at the top of the chamber, half an inch apart. The track starting on wire 2 is a proton knocked out of a deuteron. It stops in the chamber after more than one complete turn. The track starting just

above wire 10 and curving up to the right is a deuteron stopping in the chamber. The track starting above wire 11 and going down to the left is a deuteron. It is crossed by two other tracks on wire 11, both of which have nearly the same radius of curvature. These two tracks pass through the center of the lighted region but still appear less dense than the deuteron track. This means that they are protons and implies that the deuteron track is a deuteron. Those tracks which show pointed or tapered ends are passing through the edge of the lighted region and can be recognized in a single picture. The stereocamera was 25 inches from the center of the chamber and the two lenses were 4-1/2 inches apart allowing the depth of a track in the chamber to be determined to within one milli-meter, and it was always possible to find enough tracks in a picture so that a proton and a deuteron passing through the center of the lighted region could be compared and identified.

Accuracy of Measurement of Angles and Energy. The measurement of angles was simplified by restricting the tracks measured to a certain group. This also had the effect of making the number of tracks observed in each angular group more nearly equal and avoided undue effort in measuring. The direc-tion of the neutron beam was indicated by a wire stretched just above the top glass of the chamber which was parallel to the neutron beam to with-in 20 minutes of arc. The pictures were reprojected through the stereo-projector used by us[18] with two changes; first, 50 mm focal length lenses were used to match those on the camera and, second, the Western Union con-centrated arc lamp type 300 replaced the type 100 because in this experi-ment the area of the cloud chamber was much larger, and since it was repro-jected at life size it was necessary to use more light. The dip angle α and the beam angle β shown in Fig. 5 were measured for all tracks starting in the gas unless the dip angle α lay outside the region lying between plus and minus 30 degrees. If θ is the angle between the start of a track and the neutron beam, then $\cos \theta = \cos \alpha \cos \beta$. The data is analyzed into groups contained in ten degree intervals in θ and the second row of Table I shows the solid angles contained in these ten degree groups where α lay between plus and minus 30 degrees. The last row of Table I shows weighting factors which when multiplied by the number of particles observed in a ten degree group gave the best estimate of the number which would have been measured if all angles of dip had been included. The weighted numbers were used for normalization.

The energies of the protons and deuterons were determined at low energies by the range and at high energies by the Bρ of the particles. A 38 cm track corresponds to a 2 Mev proton and a 4 Mev deuteron while a 2 cm track corresponds to a 0.45 Mev proton and a 0.9 Mev deuteron. It was impossible to be sure of the identity of a track shorter than 2 cm and accordingly, those shorter than 2 cm were not measured. Above 2 Mev for a proton, the energies were determined by measurement of Bρ and the accuracy of the measurements varied, being plus or minus 10 percent up to about 4 Mev, plus or minus 5 percent from 4 to 20 Mev, and plus or minus 4 percent from 20 Mev on up. The error due to turbulence and gas scattering was negligible compared with the error in measuring the tracks with the templates, except in the case of the highest energy deuterons for which the error in measure-ment was small but turbulence increased the error giving the plus or minus

4 percent. The error in determination of the magnetic field was less than one percent.

The dip angles and beam angles were accurate to within plus or minus 1.5 degrees, allowing one degree for measurement error and half a degree for systematic error in alignment. The angle θ has an error close to plus or minus 2 degrees, but this error usually lies nearer 1.5 degrees, and particularly so at large beam angles.

The greatest inaccuracies occur where the angle and energy of a deuteron are used to determine the energy of the neutron striking the deuteron. If E is the energy of the neutron, then the estimated probable error is $\Delta E/E = 0.67 \; [(2\Delta H/H)^2 + (2\Delta\rho H/\rho H)^2 + (4 \tan \alpha\Delta\alpha)^2 + (2 \tan \beta\Delta\beta)^2]^{1/2}$. The first two terms give 0.0079 and the maximum value of the third term is 0.0014 because α cannot exceed 30 degrees. As long as β stays small, the probable error in the energy will be about 7 percent, but when β increases, the maximum error in the energy determination of the elastically scattered deuterons increases as shown in Table II. At the same time, the deuterons reduce in energy and finally get too short to measure at 0.44 Mev where they are 2 cm in length. The third column in Table II shows the energy of a neutron just sufficient to produce an elastically scattered deuteron 2 cm long at the angle β where α is zero. These are increased slightly when α is not zero, but are exact if the total angle between the deuteron and the neutron beam is used in place of the angle β.

Results. 1. Elastically Scattered Deuterons. The deuterons scattered elastically were measured for all angles where α, the angle of dip, was less than 30 degrees and the data is presented in Table III showing deuterons scattered in ten degree groups from neutrons of all energies. The upper right hand corner of the table corresponding to low energy neutron scattering at large angles shows no deuterons because the low energy of the scattered deuterons makes them unobservable. Errors at the large angles account for energies higher than the 125 Mev which is the maximum energy expected for the neutrons. In Table IV the number of elastically scattered deuterons is weighted for the different angular groups to take into account the limited solid angle observed, and Fig. 2 is a graph of the number of weighted elastically scattered deuterons plotted against the energy of the neutrons. The increase at very low energies is due mostly to neutrons of energies less than 5 Mev and the curve begins to rise again markedly at about 45 Mev. The angular distribution of those deuterons produced by neutrons with energies greater than 45 Mev is shown in Fig. 6, and this curve shows a definite narrow peak in the forward direction, which is predicted by G. F. Chew[10,11] and arises from the fact that the incoming neutron can take the proton away from the original deuterium nucleus when the proton possesses the appropriate momentum. The peak at large angles arises from the fact that in glancing collisions not enough momentum is transferred to break up the deuteron. It is possible to calculate the number of deuterons scattered at the large angles from theory and this number is larger by a factor of two than the observed number in the angular group between 80 and 90 degrees for the obvious reason that the tracks made by the scattered deuterons from neutrons are too short to measure from 85 degrees on. The total number of elastically scattered deuterons properly

weighted came to 1098.3 and to this is added 190.0 deuterons to take into account those missing from 85 degrees on. This is done for the purpose of normalizing and gives a total of 1288.3 elastically scattered deuterons.

2. Inelastic Protons. Many protons appear in the pictures and their energy distribution gives evidence of two groups, one at high energy and one at low energy merging into each other in between. The high energy group should lie in the forward angles and should appear similar to the neutron-proton scattering angular distribution except that the Pauli exclusion principle reduces the sharpness of the peak. This occurs because the original neutron for a head-on collision with the proton in the deuteron would be left right next to the neutron in the deuteron, and this is impossible if their spins are oriented in the same direction. As the angle increases, this peak of protons should decrease in energy, and Fig. 7 shows the behavior of this high energy peak. As predicted by Chew, the peak moves down in energy finally merging with the low energy peak at angles greater than 50 degrees.

The low energy peak arises from those protons which are left behind when the neutron is removed suddenly from the deuteron. These protons should have maximum energies of a few Mev, and there should be a group going backwards fewer, but comparable, in number to the low energy group going forward. Table V shows 150.4 total weighted protons going backward, all with energies below 10 Mev, while there are 404.7 protons in the same energy group going forward.

3. Cross Sections. Normalization of the data in this experiment is achieved by taking the total number of weighted protons and deuterons plus the correction in the number of deuterons in the 80 to 90 degree interval and equating this number to the total cross section for deuterium of 0.117 ± 0.005 barns measured in the neutron beam by Cook, McMillan, et al[19]. Their cross section was measured using the reaction $C^{12}(n,2n)C^{11}$ neutron induced activity which has a constant cross section above 60 Mev, possibly a peak at 40 Mev, and certainly zero below 20 Mev. Therefore it is appropriate to neglect the effect of neutrons of 20 Mev or less and it is probably reasonable to consider only neutrons above 45 Mev as being responsible for most of the 0.117 barns. In order to normalize properly only those events which were produced by neutrons of energies greater than 45 Mev should be included. The method of selection is obvious in the case of elastically scattered deuterons and Fig. 2 shows the distribution in energy of the neutrons producing the deuterons. But in the case of the inelastic protons, the method of selection demands an explanation. Below 14 Mev the neutrons do not break up the deuteron[4] any appreciable fraction of the time and this cross section for inelastic scattering should remain small for somewhat higher energies. As can be seen from Fig. 2 the number of neutrons in the interval between 14 Mev and 45 Mev is a small fraction of those at higher energies, and this coupled with the small cross section for inelastic scattering makes it seem reasonable to neglect any error that may arise from including all the protons observed in the total cross section number. With these assumptions it is possible to state the cross sections for the various processes and they are listed in Table VI. The angular distribution of the deuterons and the protons is shown in Fig. 6 in millibarns per steradian. The marked forward peak in the deuteron curve

is accurately predicted by G. E. Chew[20]. The flattening of the top of the proton curve is caused by the competing elastic deuteron scattering at small angles. The errors shown on the curves are statistical errors obtained by dividing the value by the square root of the number of particles actually observed.

Comparison with Other Experiments. The cross section for the scattered protons going in the forward direction can be compared with the n-p cross section. As indicated earlier, these cross sections should be nearly equal at angles around 40 degrees but the strong peak at zero degrees in the laboratory system for n-p scattering should be greatly reduced for the scattered protons from deuterium. The dotted curve in Fig. 8 is the n-p scattering cross section for 90 Mev neutrons as obtained by Hadley et al.[17], and the solid curve gives the angular distribution of the protons from deuterium and illustrates the flatness of the peak in the forward direction. The proton curve in both Fig. 6 and 8 is taken from data given in Table V in the row marked "protons produced by neutrons with energies greater than 45 Mev." These were selected so as to exclude the protons with low energies left behind when the neutron is removed suddenly. If the proton energy was less than 45 cos θ Mev it was not included in this graph.

A. L. Bloom and M. O. Stern[21] measured the differential cross section for elastic scattering of 190 Mev deuterons on protons and obtained an angular distribution which should agree with the angular distribution of the elastically scattered deuterons in our experiment if the n-n cross section and the n-p cross section are the same at high energies. Fig. 9 shows the results obtained by Bloom and Stern compared with the n-d elastic cross section, and the agreement is surprisingly good considering the errors which may be present in determination of the absolute cross sections. These errors are difficult to estimate and depend upon the accuracy of the total cross section of 117 millibarns for 90 Mev neutrons on deuterium[19]. The indication is that n-n and n-p cross sections at this energy are the same.

Conclusion. The scattering of deuterons by 90 Mev neutrons is divided between inelastic and elastic events in a way predictable by the theory developed by G. F. Chew and others. The elastic collisions show a sharp forward peak due to the pickup of a proton by the incoming deuteron. The protons fall into two groups, high energy protons in the forward direction and low energy protons which tend to be spherically symmetric. The forward peak of protons is weaker at small angles than would be explainable on the basis of n-p scattering alone. This is explained by the application of the Pauli principle to the two remaining neutrons.

References:

[1] H. H. Barschall and M. H. Tanner, Phys. Rev. 58, 590 (1940)
[2] J. H. Coon and H. H. Barschall, Phys. Rev. 70, 592 (1946)
[3] M. Ageno, E. Amaldi, D. Bocciarelli, and G. C. Trabacchi, Nuovo Cimento 9, i (1943); Phys. Rev. 71, 20 (1947).
[4] J. H. Coon and R. F. Taschek, Phys. Rev. 76, 710 (1949).
[5] J. F. Darby and J. B. Swan, Aust. Jour. Sci. Res. A, 1, 18 (1948).
[6] S. L. Martin, E. H. S. Burhop, C. B. Alcock, R. L. F. Boyd, Proc. Phys. Soc. A, 63, 884 (1950).
[7] G. L. Griffith, M. E. Remley, P. C. Kruger, Phys. Rev., 79, 443 (1950).
[8] R. A. Buckingham and H. S. W. Massey, Proc. Roy. Soc. A, 179, 123 (1941).
[9] H. S. W. Massey and R. A. Buckingham, Phys. Rev. 71, 558 (1947).
[10] Geoffrey F. Chew, Phys. Rev. 74, 809 (1948).
[11] Geoffrey F. Chew, Phys. Rev. 80, 196 (1950).
[12] H. York, Phys. Rev. 75, 1467A (1949).
[13] J. Hadley and H. York, Phys. Rev. 80, 345 (1950).
[14] K. Brueckner and W. M. Powell, Phys. Rev. 75, 1274 (1949).
[15] R. Serber, Phys. Rev. 72, 1007 (1947).
[16] W. M. Powell, Rev. Sci. Instr. 20, 402 (1949).
[17] Hadley, Kelly, Leith, Segrè, Wiegand, and York, Phys. Rev. 75, 351 (1949).
[18] Brueckner, Hartsough, Hayward, and Powell, Phys. Rev. 75, 555 (1949).
[19] Cook, McMillan, Peterson, and Sewell, Phys. Rev. 75, 7 (1949).
[20] Geoffrey E. Chew, Phys. Rev. 1951.
[21] A. L. Bloom and M. O. Stern, Bull. Am. Phys. Soc. 25, No. 6, J-6.

TABLE I

Angular of Interval θ_1-θ_2 in Degrees	0-10	10-20	20-30	30-40	40-50	50-60	60-70	70-80	80-90
Solid angle between θ_1 and θ_2 $-30^\circ \leq \alpha \leq 30^\circ$	.0954	.283	.469	.436	.386	.376	.375	.366	.367
Solid angle between θ_1 and θ_2 for all α's	.0954	.283	.469	.628	.768	.897	.999	1.052	1.091
Weighting factors	1	1	1	1.44	1.99	2.39	2.66	2.88	2.98

TABLE II

Beam angle β in degrees.	Maximum fractional error in the energy	Energy of a neutron in Mev for a deuteron track 2 cm long.
0	0.067	.5
30	0.075	.7
50	0.095	1.1
65	0.137	2.8
75	0.218	7.4
80	0.322	16.5
82	0.40	26.1
84	0.53	45
85	0.64	65

TABLE III

Elastically Scattered Deuterons

Neutron Energy	0-10°	10°-20°	20°-30°	30°-40°	40°-50°	50°-60°	60°-70°	70°-80°	80°-90°
0-1	8	13	7	1	4	0	0	0	0
1-2	8	34	27	14	11	1	0	0	0
2-3	3	17	18	10	8	6	0	0	0
3-4	3	9	10	3	4	2	1	0	0
4-5	0	3	5	1	4	5	2	0	0
5-6	4	4	2	2	3	2	1	0	0
6-7	1	3	4	1	0	1	2	0	0
7-8	0	2	2	0	1	0	4	0	0
8-10	0	3	5	3	2	2	5	0	0
10-12	0	1	0	1	0	2	1	1	0
12-14	0	1	0	0	2	2	1	3	0
14-20	2	2	2	1	1	1	6	3	3
20-30	4	3	4	7	4	1	7	5	2
30-40	1	5	5	5	1	3	5	6	0
40-45	1	8	3	2	2	2	1	3	1
45-55	7	12	7	3	4	3	7	13	5
55-65	1	8	7	3	3	5	13	19	9
65-75	5	8	4	6	4	7	18	25	12
75-85	3	7	10	7	3	8	18	30	10
85-95	5	6	2	5	5	8	12	16	9
95-105	1	2	0	1	3	7	10	9	6
105-115	1	0	1	1	3	2	4	9	6
115-125	1	0	0	1	1	3	4	6	2
125-135	0	0	0	0	0	2	1	2	1
135-145	0	0	0	0	0	0	1	2	1
145-175	0	0	0	0	0	0	0	0	3

TABLE IV

Weighted Elastically Scattered Deuterons

Neutron Energy	0-10	10-20	20-30	30-40	40-50	50-60	60-70	70-80	80-90	Total
0,5	22	76	67	41,7	27,8	33,5	8,0	0	0	276,0
5-10	5	12	3	8,6	11,9	12,0	31,9	2,9	0	87,3
10-14	0	2	0	1,4	4,0	9,6	5,3	11,5	0	33,8
14-20	2	2	2	1,4	2,0	2,4	15,9	8,7	8,9	45,3
20-30	4	3	4	10,1	8,0	2,4	18,6	14,4	6,0	70,5
30-40	1	5	5	7,2	4,0	7,2	13,3	17,3	0	60,0
40-45	1	8	3	2,9	4,0	4,8	2,7	8,6	3,0	38,0
45-55	7	12	7	4,3	8,0	7,2	18,6	37,4	14,9	116,4
55-65	1	8	7	4,3	6,0	12,0	34,6	54,7	26,8	154,4
65-75	5	8	4	8,6	8,0	16,7	47,9	72,0	35,8	206,0
75-85	3	7	10	10,1	6,0	19,1	47,9	86,4	29,8	219,3
85-95	5	6	2	7,2	9,9	19,1	31,9	46,0	26,8	153,9
95-105	1	2	0	1,4	6,0	16,7	26,6	25,9	17,9	97,5
105-115	1	0	1	1,4	6,0	4,8	10,6	25,9	17,9	68,6
115-125	1	0	0	1,4	2,0	7,2	10,6	17,3	6,0	45,5
125-135	0	0	0	0	0	4,8	2,7	5,8	3,0	16,3
135-145	0	0	0	0	0	0	2,7	5,8	3,0	11,5
145-175	0	0	0	0	0	0	0	0	8,9	8,9
Total 45-175	24,0	43,0	31,0	38,7	51,9	107,6	234,1	377,2	190,8	1098,3

190,0 deuterons added for those of too low energy to be identifiable.

1098,3
190,0

Total elastically scattered deuterons from neutrons of greater than 45 Mev.   1288,3

TABLE V

Inelastically Scattered Protons

Angular Interval	0-10°	10-20°	20-30°	30-40°	40-50°	50-60°	60-70°	70-80°	80-90°	90 →	Total
Protons with energies greater than 10 Mev	75	223	299	159	103	81	42	24	10	4	
weighted	75	223	299	228.6	205.0	193.5	111.8	69.0	29.8		1434.7
Protons with energies less than 10 Mev	8	18	29	20	32	22	23	29	22	73	
weighted	8	18	29	28.8	63.6	52.5	61.2	83.5	65.5		410.1
Angular Interval	180-170	170-160	160-150	150-140	140-130	130-120	120-110	110-100	100-90		
Protons going Backward	2	7	9	5	13	6	12	8	11		
weighted	2	7	9	7.2	25.8	14.3	31.9	23.0	32.8		153.0
											1997.8
Angular Interval	0-10°	10-20°	20-30°	30-40°	40-50°	50-60°	60-70°	70-80°	80-90°	90 →	
Protons of more than 10 Mev from Neutrons of more than 45 Mev energy.	60	187	238	139	80	76	42	24	10		
Millibarns per steradian	22.4	23.5	18.1	11.5	7.4	7.5	4.1	2.2	0.9		

TABLE VI

Kind of Event	Weighted Number of Events	Cross Section in Millibarns
Elastically scattered deuterons from neutrons with more than 45 Mev.	1288.3	45.9
Protons going backwards	153.0	5.4
Protons with more than 10 Mev	1434.7	51.1
Protons with less than 10 Mev	410.1	14.6
Total of all kinds	3286.1	117.0
Inelastically scattered protons		71.1
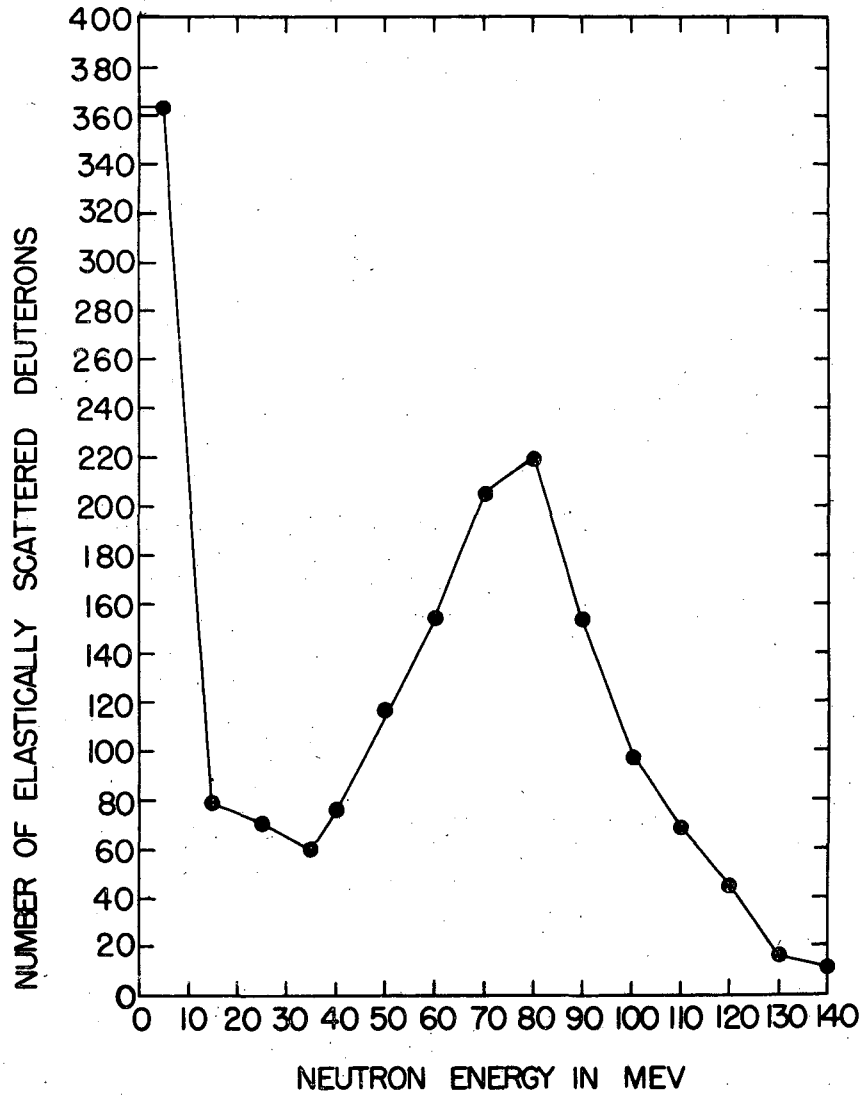
Fig. 2. -The number of elastically scattered deuterons plotted against the energy of the neutrons in Mev
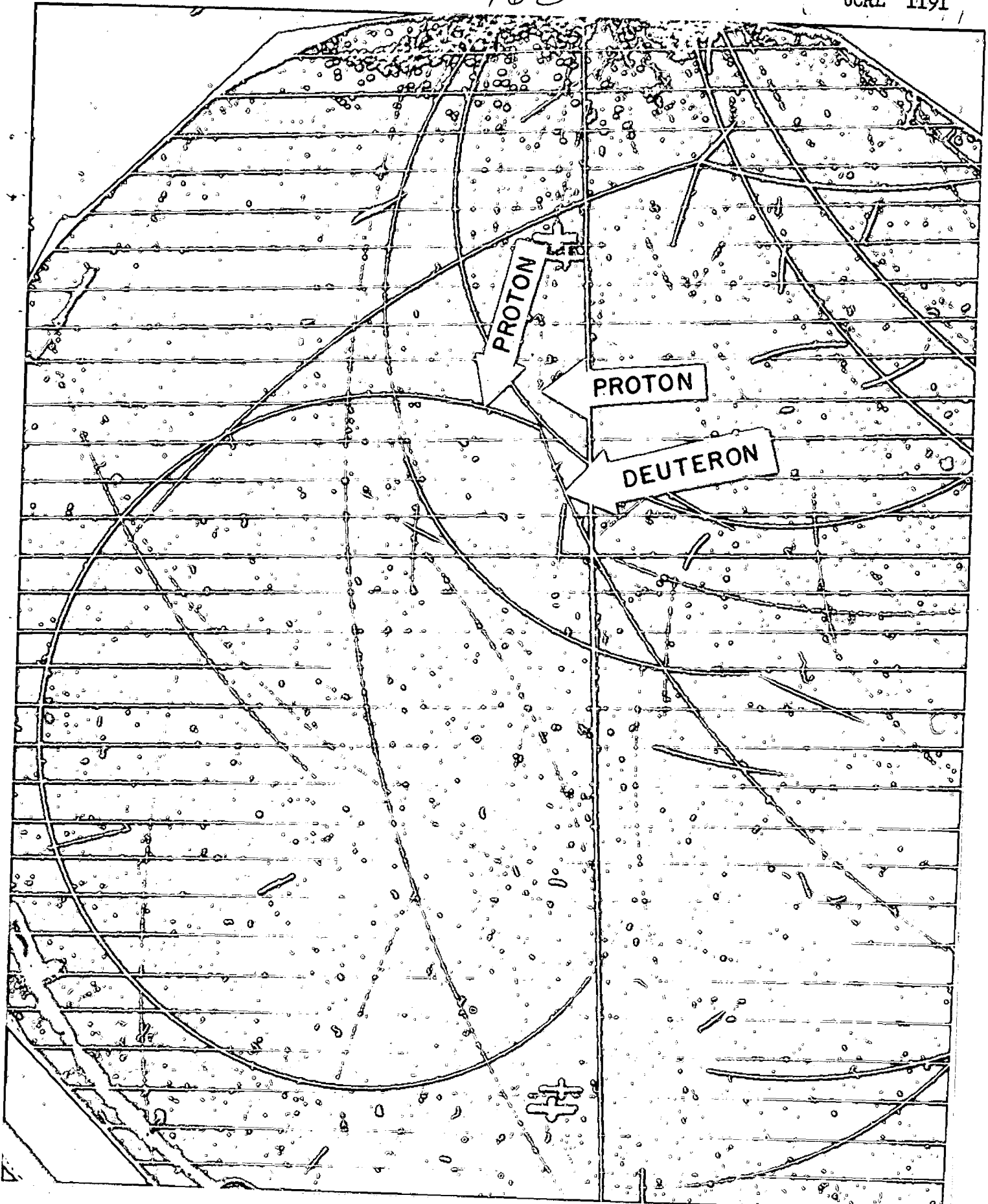
Fig. 3 - A proton, marked by the arrow, is knocked out of the window of the cloud chamber and collides with a deuteron in the gas of the chamber. The proton recoils backwards and to the left. The deuteron goes ahead with momentum equal to the change of momentum of the proton, but with heavier ionization showing that it is a deuteron.
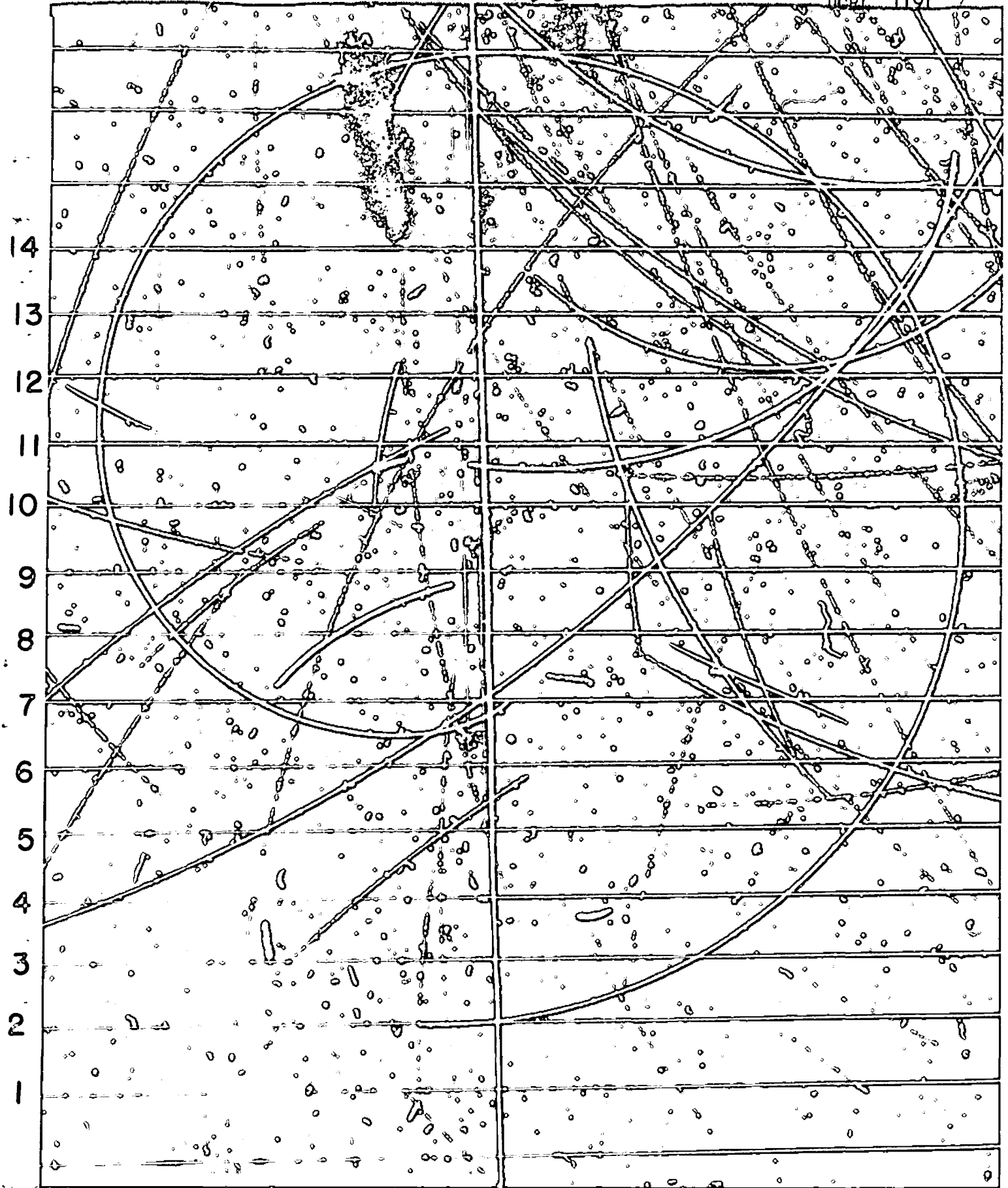
Fig. 4 - The neutron beam runs from top to bottom parallel to the vertical wire. The horizontal clearing-field wires are numbered. The track starting above wire 13 to the left of the vertical wire is a proton, the track starting just above wire 11 is a deuteron, the track starting just above wire 10 is a deuteron, the one just above wire 8 is a deuteron, the one just above 7 is a proton, and the long spiral starting on wire 2 is a proton.
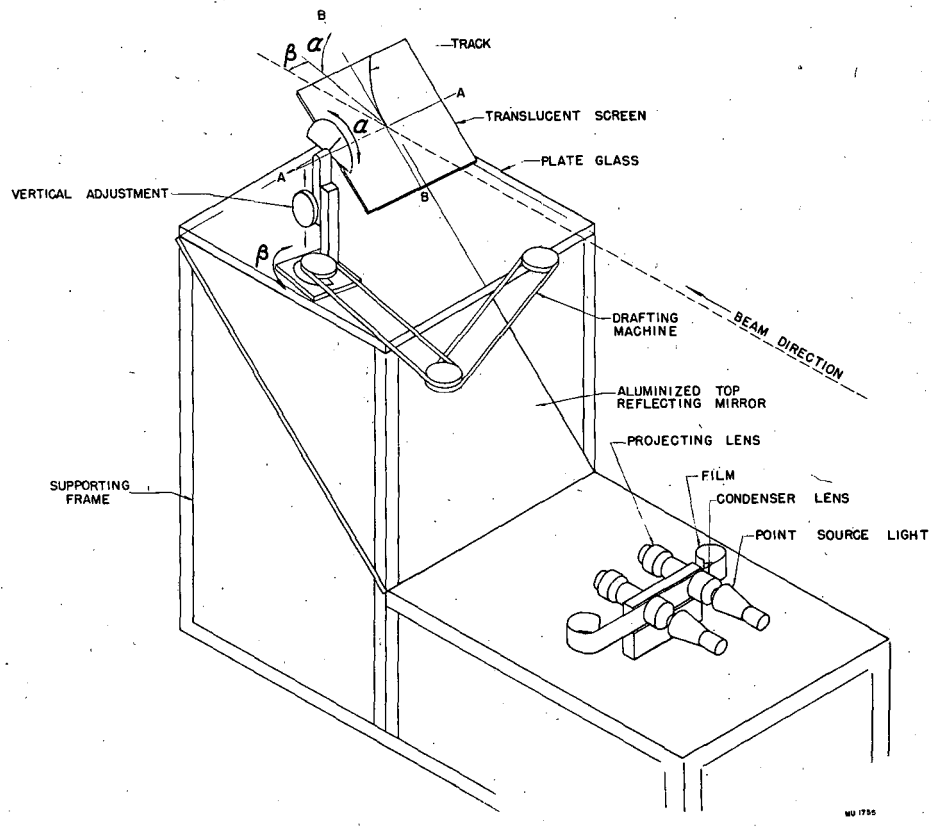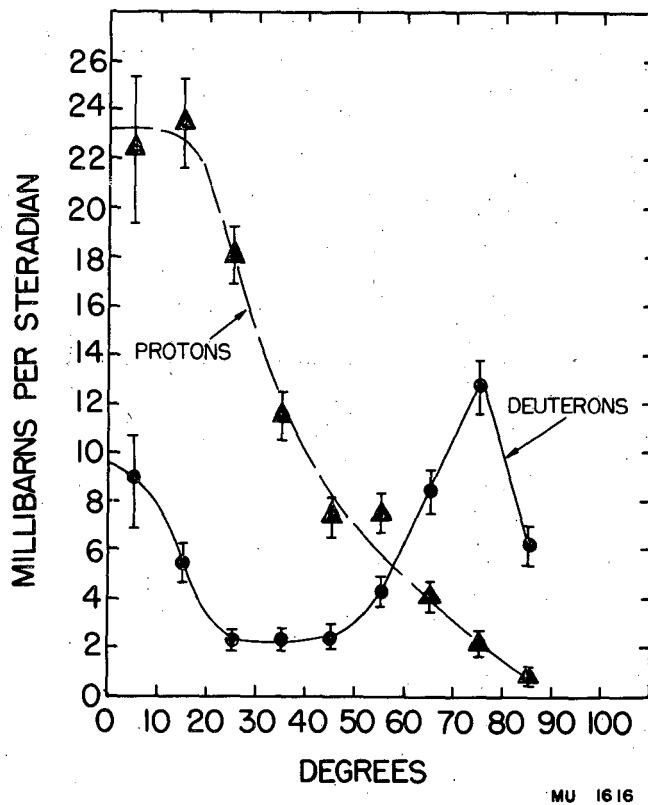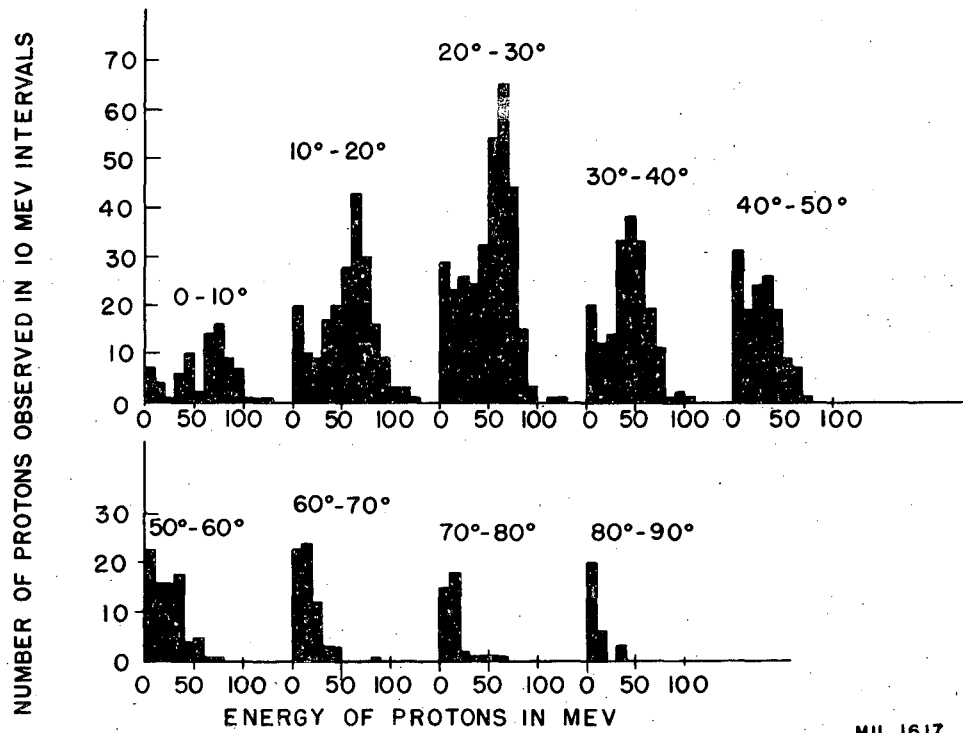
ZN-31

Fig. 5 - A schematic drawing of the reprojection apparatus.

16 f

Fig. 6 - The angular distribution of the deuterons scattered by neutrons
of energy greater than 45 Mev is given by the circles. The angular distribution for
for protons scattered directely by 90 Mev neutrons is given by the circles
with crosses.

Fig. 7 - The energy distribution of the scattered protons in angular intervals of 10 degrees.
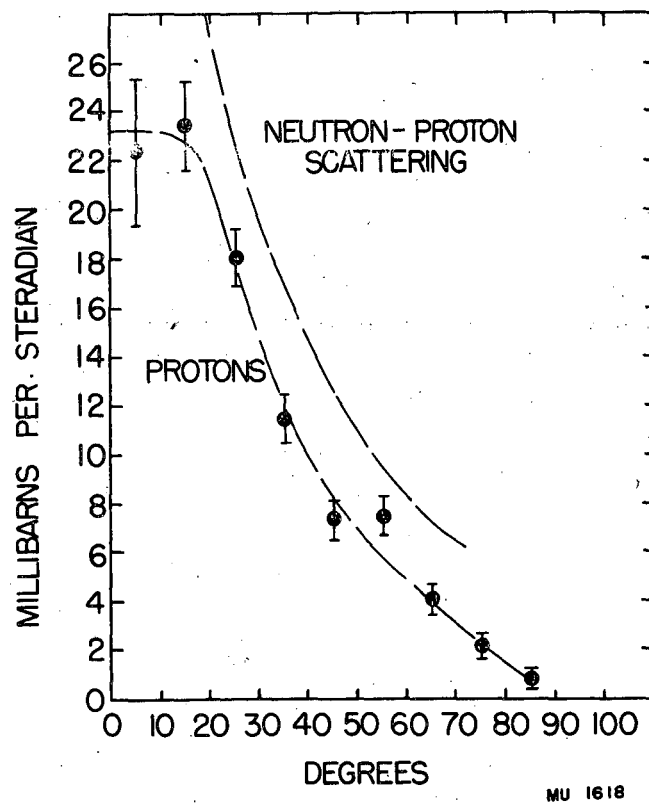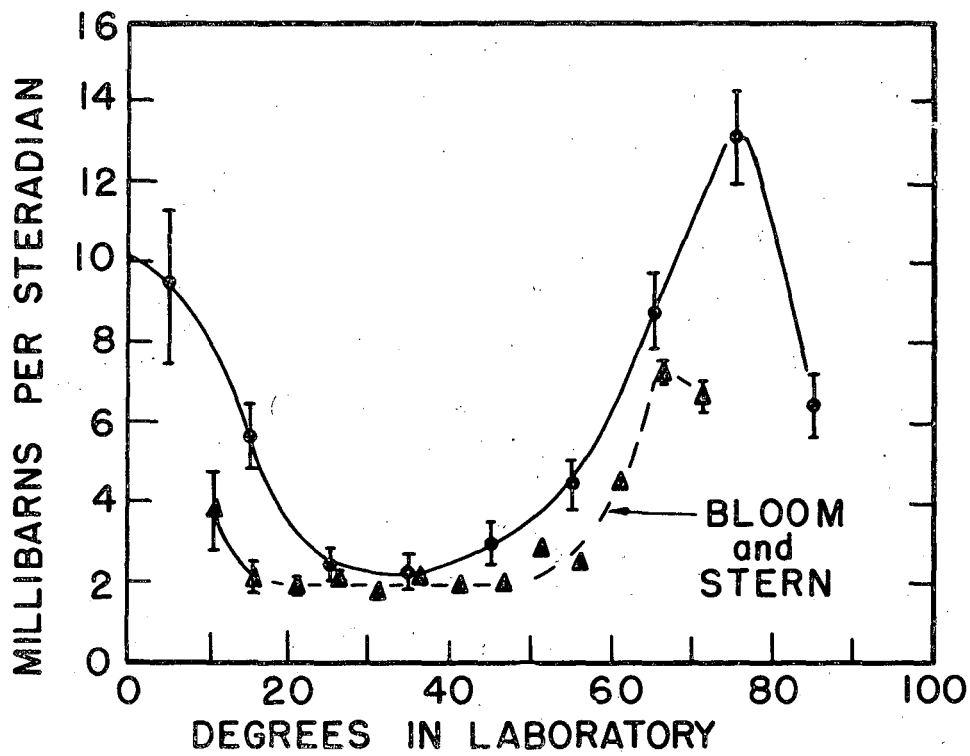
MU 1618

Fig. 8 - Comparison of the angular distribtuion of the inelastically scattered protons from deuterium with that for protons scattered directly by 90 Mev neutrons.

MU 1619

Fig. 9 - Comparison of Bloom and Stern's results with the angular distribution of elastically scattered deuterons.

2. Film Program

Walter H. Barkas

High Energy Electron Processes. (W. Barkas, C. Violet, F. Gilbert, R. Deutsch, L. Germain) The events occurring along the path of 200 Mev and 300 Mev electrons and positrons have been studied by passing the particles through sensitive emulsion in which the old electron tracks have been erased by an accelerated fading technique. By this means the absolute cross sections for electron-electron and positron-electron scattering, pair production in the fields of nuclei, and nuclear scattering can be measured.

Positron-electron and electron-electron scattering events occur frequently and hundreds of such collisons have been recorded. In the preliminary study, which has been completed, agreement with the theoretical cross section was found for knock-on particles of energies in the range 30-150 Kev, but a deficiency of high energy knock-ons was found. This result is rather surprising since the theory of the scattering is believed to be sound. A more exhaustive study of the high energy knock-ons is now in progress, and a check has been made of the energy of the primary particles by small angle scattering. The small angle scattering verifies the assumed energy. Studies of processes other than scattering by electrons in the emulsion have not been completed.

Meson Masses (W. Barkas, F. Smith, E. Gardner) A phase of the program of meson mass measurement has been completed and the following manuscript sent to the Physical Review as a letter: "Meson to Proton Mass Ratios", Barkas, Smith and Gardner. An extended series of measurements has been made on the ratios of meson masses to the mass of the proton. As in our previous work[1] momenta and ranges of the mesons were measured, but a number of improvements over our earlier procedures have been devised to reduce systematic errors. Using prior knowledge of the approximate mass ratios, protons and mesons from separate targets in the 184-inch cyclotron were magnetically selected so as to lie in the same 5 percent velocity interval. The particles were stopped in the same nuclear emulsion which they entered at a small angle to the surface. Relative momenta were calculated with errors of less than a part per thousand for the orbits[2], which are approximately semi-circular. The rectified ranges in emulsion of the particles were carefully measured. For a small interval, the range-momentum relation is well represented by a power law: $R/m = c(p/m)^q$, where R is the range, m the particle mass, p the momentum, and c a constant of the emulsion. We have used the exponent $q = 3.50$ derived from the range-energy relation[3]; the results, however, are insensitive to the value of q chosen. The utilization of protons with velocities distributed about the average meson velocity enabled us to evaluate c, and only momentum and range ratios entered into the determination of the mass ratios. Since all the particles are stopped in the same body of nuclear emulsion, the stopping power of the emulsion is eliminated. The momentum ratios are independent of the absolute value of the magnetic field intensity.

Other statistical errors are small in comparison to the range straggling error of an individual observation. We have observed that for monoenergetic (π-μ decay) particles the straggling of ranges has closely a normal distribution. The most probable mass is therefore obtained by averaging the individual observations of that function of the mass in which the range occurs linearly (i.e. $R/p^{3.5}$).

We find the following mass ratios

$$\frac{\pi^+}{\text{PROTON}} = 0.1511 \pm 0.0006$$

$$\frac{\pi^-}{\text{PROTON}} = 0.1504 \pm 0.0007$$

Particles[4] which were presumed to be μ^+ mesons originating from decay of π^+ mesons stopping in the target were measured in the same experiment. The dispersion of apparent masses in this case, however, exceeds that to be expected if the particles were representatives of a single mass group all of which come from the target. μ^+ mesons which arise from decay of $\pi+$ mesons in flight doubt-less contribute to the distribution found, and we therefore must defer quoting a new μ^+ mass measurement until a better separation of the groups is obtained.

A reliable value for the μ^+ meson mass was not obtained in this experiment, so that another measurement of it is now under way.

Energetics of π Meson Decay (W. Birnbaum, F. Smith, W. Barkas). μ meson ranges from the decay of π mesons have been measured in emulsion which was calibrated using π mesons of accurately known momentum. Assuming π and μ masses, this experiment yields the mass of the neutral particle taking part in the $\pi-\mu$ decay. An accurately known μ^+ mass is not yet available, however, so that no results on the neutral particle mass can be given yet.

One very anomalous range of a μ meson was found. This suggests that there may be more than one process taking place in the π decay.

If the decay of π mesons in flight is studied, further information should be obtainable, and two of the three masses, π, μ and ν are calculable in terms of the other. Such an experiment is contemplated.

Branching Ratio of π Meson Decay. (F. Smith). This program was completed and the following manuscript was submitted to the Physical Review as a letter to the editor: "On the π^+ Branching Ratio", F. M. Smith. Early experiments on π^+ mesons, using photographic emulsions as detectors, have seemed to show[5] that some of the π^+ mesons, upon stopping in matter, do not decay into μ^+ mesons.

These studies were concerned with mesons of fairly low energy so that the emulsion would be the only stopping material. Ilford C2 and C3 emulsions were used in order to facilitate the identification of the mesons. In many cases the processed emulsions showed an apparent non-uniformity in sensitivity and since the μ meson track is rather tenuous in the region of the terminus of the π track, there is a chance of missing the decay. For a more intensive study of the decay scheme, a much more sensitive emulsion is required. Ilford G5 and Eastman NTB3 emulsions were chosen for the present study.

The apparatus used in this study consisted of a brass chamber for hold-ing the plates and the target, as shown in Fig.1. The target was 0.036-inch

carbon. This assembly was mounted on a probe and inserted into the vacuum chamber of the 184-inch cyclotron. The circulating beam of 345 Mev protons irradiated the target. Mesons emitted in the backward direction entered a channel cut into the brass holder. This channel was of such dimensions that π^+ mesons from the target with energies between 6 and 8 Mev only will enter the emulsion after a turn of 180°. No μ mesons from decay of the π stopping in the target can get into the plate chamber. μ mesons from decay in flight of the π mesons could get into the emulsion only if they were emitted in a narrow cone in the forward or backward direction. These would not be confusable with π mesons from the target as their ranges in the emulsion would be too great or too small to have the correct energy.

The plates were studied using a high power microscope. Only those mesons which stopped in the emulsion at a distance greater than 10 microns from either surface of the undeveloped emulsion were counted.

Meson scattering from the channel walls gave a background fairly uniformly distributed with respect to range in the emulsion.

Analysis of results consisted of calculating the number of background μ mesons expected to fall in the main distribution. This number was subtracted from the number of mesons showing no decay found in the main distribution.

A preliminary estimate of the percentage of π mesons from the target which do not decay into μ mesons is: $R = 0.3 \pm 0.4$ percent. This indicates that the branching ratio of the π^+ mesons is less than 1 percent and probably zero. A more complete account of this work will be published at a later date.

Range Straggling (F. Smith, W. Birnbaum, W. Barkas). The decay of the π^+ meson provides a monoenergetic source of μ mesons, and a study of the distribution of their ranges yields data for comparison with the theory of straggling. The emulsion is particularly valuable for this sort of study because the whole path of the particle is visible; the true rectified range can be measured, and the effect of scattering separated out. μ mesons in three nuclear emulsion plates have been studied. The ranges and the standard deviations of the ranges have been measured. The normality of the straggling distribution has been tested. In general the predictions of theory are verified. The "geometrical straggling" arising from scattering of the particles has also been measured.

Large Angle Scattering and Stars Produced by Fast π Mesons in Nuclear Emulsion (H. Bradner, B. Rankin). An investigation has been completed of the scattering and other nuclear interactions of energetic π^- mesons in emulsion. Mesons of approximately 38 Mev were obtained by a channel inside the cyclotron. These mesons traverse G5 emulsion. Four hundred and six hundred micron emulsions were placed with their surfaces parallel to the meson beam, so that individual meson tracks could be followed. Mesons were differentiated from protons by their grain density and small angle coulomb scattering in the first 500 microns of observed track. μ-meson background was determined by observing tracks in a second set of emulsions placed beyond the range of the π^- mesons. Scatters between 5° and 25° are in agreement with single coulomb scattering. Eleven scatters of total angle greater than 90° and 11 stars were observed in a total length of 902 ± 30.4 cm of π^- meson track. Five mesons were seen to disappear in flight. The latter events may be attributed to the reaction $\pi^- + p \longrightarrow \pi^0 + n$ or to "stars" with only neutrons emitted. The mean free paths for scatters

greater than $90°$, stars, and total nuclear interaction are, respectively, 82.0 ± 16.9, 82.0 ± 16.9, and 23.7 ± 3.2 cm. Total nuclear interaction is computed by assuming isotropic nuclear scattering. Nuclear area of the elements of the emulsion corresponds to approximately 23 cm mean free path. Hence, it appears that the total cross section for nuclear interaction of 30-40 Mev π^- mesons in emulsion is equal to nuclear area. A similar experiment using π^+ mesons has been begun.

Meson Scattering in Pure Materials (H. Heckman, W. Barkas, K. Bowker). Continued work on meson focusing inside the cyclotron has shown that about 20 π^- mesons/sq cm/Mev/sec in the vicinity of 45 Mev is about the maximum available intensity in a collimated beam. A preliminary scattering experiment was carried out using an aluminum scatterer. In view of the low meson intensity, rather poor geometry and large thickness of scatterer were used. The results were encouraging, however. Virtually no background mesons were present, and a cross section for scattering of ~ 40 Mev π^- mesons of about 5×10^{-25} sq cm was found, assuming spherical symmetry of the large angle scattering.

A better experimental arrangement was then developed for the study of scattering of π^- mesons by protons, and incidentally by carbon. Scatterers of polyethylene and carbon are used, so that the subtraction technique can be applied. The mesons scattered at $90°$ from hydrogen will suffer a 25 percent loss of energy because of the small mass of the proton. Mesons elastically scattered from carbon will not sustain a large energy loss on scattering so the two groups of mesons are separable by range, and the mesons scattered from hydrogen should be diluted only by mesons inelastically scattered from carbon and by the background from neutrons. The experiment has now been performed, but the nuclear emulsion plates used to detect the scattered mesons have not yet been analyzed.

Grain Density of Nuclear Emulsion Tracks (K. Bowker, W. Barkas and T. Green). The usefulness of the nuclear emulsion as a quantitative instrument is increased if one has reliable information on the grain density of tracks as a function of all the pertinent variables. A program of study of grain density has revealed the following for fully developed tracks:

a. The grain density is a function only of the rate of energy loss of the charged particle, and, with little qualification, is independent of the particle charge or velocity separately.

b. For low grain densities, the grain density and the rate of energy loss are proportional; at high grain densities, a saturation of grain density sets in, and the grain density no longer increases in proportion to the rate of energy loss.

c. At high grain densities, where the grain density is no longer sensitive to the rate of energy loss, the gaps in the tracks are sensitive to the rate of energy loss and the "integrated emptiness" of the track provides as good a measure of the rate of energy loss and the rate of change of energy loss as the grain count.

d. By adjusting a sensitivity factor, the grain density vs. rate of energy loss curves for the standard emulsions may be made to coincide.

μ-Meson Decay Spectrum (R. Sagane, E. Gardner, H. Hubbard). The energy spectrum of positrons from μ^+ meson decay has been studied with a technique of large solid angle focusing obtained with an axially symmetric heterogeneous magnetic field. This method has been under development at Tokyo University since 1941 and is called "The Spiral Orbit Spectrometer".

A pair of large Helmholtz coils built for a cloud chamber were used with the addition of iron cores and yokes, so that electrons of energy up to about 60 Mev originating on the axis could be focused close to the so-called "stable orbit". The electrically deflected proton beam of the 184-inch cyclotron was passed parallel to the magnet axis through a 1-1/2 inch hole in the pole piece and produced mesons in a C or Be target located on the axis in the pole gap.

Four anthracene crystals 3/4 in. x 1-1/4 in. x (15/64 in - 10/64 in.) were located 15° apart with their outer edges at the stable orbit position. Counts of quadruple coincidences were taken using five successive gates each of two microseconds duration triggered by the deflecting pulse of the cyclotron.

Some π^+ mesons produced at the target remain inside the target due to absorption and the presence of the magnetic field. The μ mesons from the decay of the π mesons usually will remain in the target. The μ mesons then decay into fast electrons which escape from the target with little loss of energy.

These electrons are then detected by the crystals after being focused by the magnetic field.

The counting rates of the five gates indicate the relative members of electrons detected in two microsecond intervals which are delayed successive multiples of two microseconds. Thus one can obtain a decay curve for μ mesons from these counts. The sum of these counts also provides the relative intensity of decay electrons in various momentum intervals.

Results obtained so far have shown that the maximum positron energy is close to 56 Mev with the intensity maximum around 40 Mev. The spectrum has the closest resemblance to the curve given by Tiomno, Wheeler and Rau[6] for tensor coupling and antisymmetrical charge exchange, assuming $\mu^+ \rightarrow 2\nu + e^+$, $\mu^+ = 210$ e.m. and $\nu = 0$. The accuracy is estimated as $\pm$ 3-4 percent in energy resolution and $\pm$ 20 percent for intensity. A further effort is being made in order to obtain an accuracy of $\pm$ 2 percent in energy and $\pm$ 10 percent in intensity so that a definite answer can be given for the choice of assumptions in the theory.

Work for Other Laboratories (W. Barkas). Numerous exposures of plates to mesons and to protons of known energies have been made for laboratories in Europe and the United States. A collaboration with a number of universities in Japan has been established whereby experiments are carried out in Berkeley, and the time consuming analysis of the plates is done by Japanese microscopists.

[1]F.M.Smith et al., Phys. Rev. 78, 86 (1950).
[2]W. H. Barkas, Phys. Rev. 78, 90 (1950).
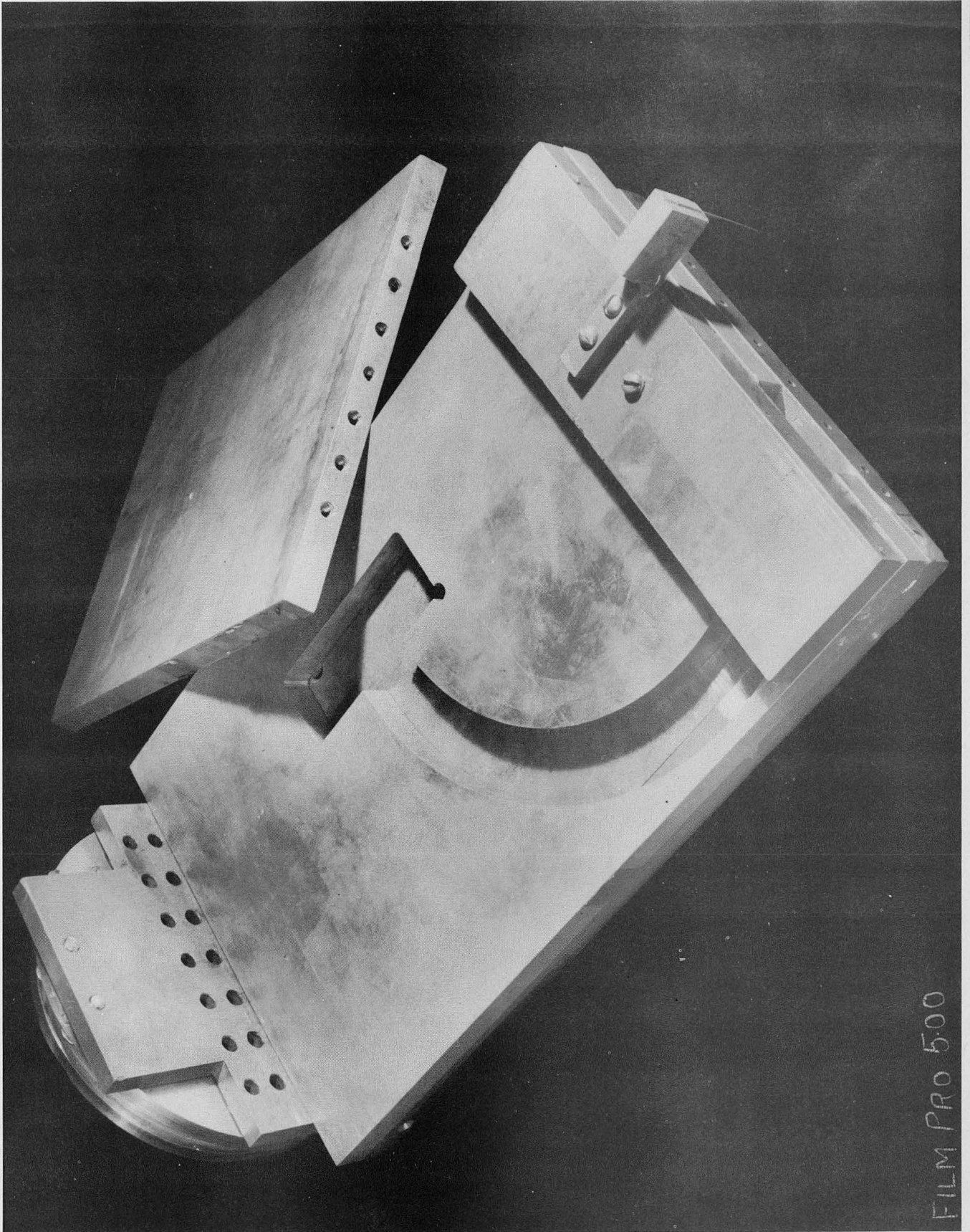[3]H. Bradner et al., Phys. Rev. 77, 462 (1950).
[4]J. Burfening, E. Gardner, and C. M. G. Lattes, Phys. Rev. 75, 382 (1949).
[5]J. Burfening, E. Gardner, and C. M. G. Lattes, Phys. Rev. 75, 383-4 (1949).
[6]Tiomno, Wheeler and Rau, Reviews of Modern Physics, Jan.(1949).

FIG. 1

3. High Energy Proton Interactions With Nuclei

J. B. Cladis, W. Hess, B. J. Moyer

Energy spectra of 340 Mev protons scattered from various nuclei have been obtained at a number of scattering angles. The spectra have been obtained by means of the 35-channel magnetic particle spectrometer reported by Hadley in an earlier quarterly report. The energy resolution of this equipment has been improved about a factor of three by the inclusion of coincidence circuits to identify particles in the 17 overlap channels. A measurement of the energy resolution of the equipment is given by the width of the proton energy spectrum from hydrogen. This is now about 30 Mev at 330 Mev using targets that are about 8 Mev thick. The energy resolution improves at lower energies.

Spectra have been obtained at $8-1/2°$, $10-1/2°$, $13°$, $15°$, and $17°$ using targets of H, C, Al, Cu, and Pb, and at $41-1/2°$ using C as target. The spectra from all of the targets except those from hydrogen, have widths which increase monotonically with scattering angle. This behavior is to be expected if one considers the problem of scattering monoenergetic particles from equal mass particles possessing arbitrarily directed momenta before collision. The solution is such that monoenergetic particles are still observed at a scattering angle of $0°$; at larger angles the energy spread of the scattered particles increases considerably. Experimentally, we find the widths of the proton spectra from carbon at $8-1/2°$, $10-1/2°$, $13°$, $17°$, and $41-1/2°$, to be 32, 34, 65, 78, and about 200 Mev respectively.

At small angles, this "quasi-elastic" scattering (nucleon-nucleon collisions) cross section is smaller than the cross section of elastic scattering from the nuclei. At angles within the first and second maxima of the diffraction scattering pattern for the elements found by Ball, Richardson, and Moyer, the spectra are peaked near the full beam energy, at energies higher than those at the peaks of the spectra from hydrogen. At larger scattering angles, the peaks of all of the spectra fall nearly at the same energy as those from hydrogen. Moreover, at angles corresponding to the minima of the diffraction scattering, the peaks of the spectra fall again at the energies appropriate to quasi-elastic scattering. We find this condition to hold at $8-1/2°$ for Pb, $10-1/2°$ for Cu, and at $15°$ for Al.

The peak of the proton spectrum from carbon at $41-1/2°$ falls about 50 Mev lower than that from hydrogen. This can qualitatively be explained by the higher cross sections for collisions involving lower relative incident momenta particles; by the averaging of the scattered proton energies from target nucleons with all possible initial directions; and by the energy requirements for the nuclear transformation involved, for example, $C^{12}(p,2p) B^{11}$ requires about 20 Mev.
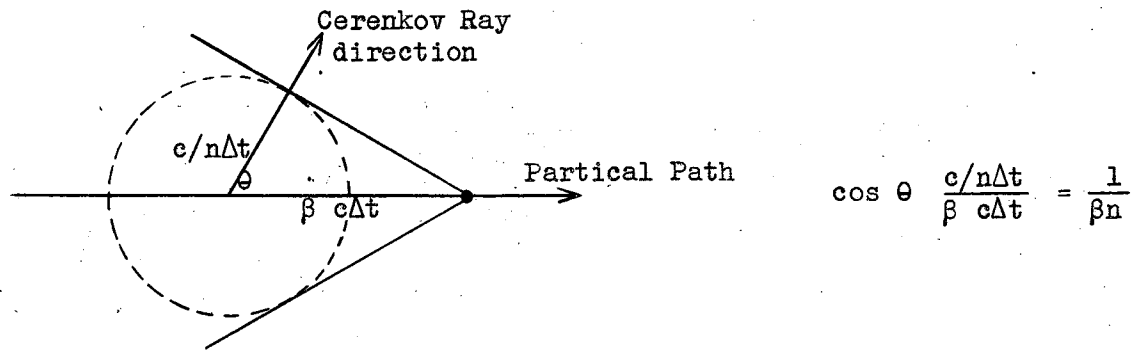
4. Measurement of Proton Energy by Cerenkov Radiation

R. L. Mather

The observation of Cerenkov radiation from protons has been previously described in UCRL-409. These experiments which were similar to some which had been done earlier with electrons[1] corroborated the general correctness of the Frank and Tamm theory[2] for the angular distribution and total intensity of this radiation.

The theory predicts an angular distribution as sharp as a delta function in the directions making an angle Θ with the path of the charged particle. The angle Θ is related to the index of refraction, n, of the medium and the velocity of the particle, $\rho = v/c$, by a formula derivable from very elementary considerations. If Θ and n can be measured then the velocity of the particle is determined. From this the energy of the particle can be calculated if its mass is known.

Cerenkov radiation is essentially an electromagnetic shock wave excited by the passage of a charged particle through the medium with a velocity greater than the velocity of electromagnetic radiation in the medium. The wavefront is a cone with its apex at the particle whose rays propagate in a direction making an angle Θ with the particle path. A brief consideration of the following diagram yields the relation on which the following measurements are based. The particle initiated a Huygens wavelet at time Δt ago which has now reached a radius of (c/n) Δt while the particle has traveled ahead a distance β cΔt. By trigonometry the relation follows

Cerenkov Ray direction

c/nΔt

Partical Path

β cΔt

$$\cos \Theta \quad \frac{c/n\Delta t}{\beta \; c\Delta t} = \frac{1}{\beta n}$$

Further considerations show that n is strictly the index of refraction even in dispersive media although here Θ will depend on the wave length of the light since n is a function of the wave length.

The earlier pictures did not define Θ well enough to be particularly useful for proton energy measurement. It was realized that the loss of definition came from three principal sources 1. Crude optical work 2. Scattering of the particles in the material 3. The dispersion of the glass.

The scattering was reduced by using a much thinner layer of material (about 2/3 mm instead of 10 mm thick) and a picture taken with an improved optical system is shown in Fig. 1 along with a scale of Θ.

This picture was taken by an ordinary camera looking in through the polished surface of the material. What it should see is a limited portion of a circular rainbow of light centered on the direction of the incoming proton beam with the blue outside and the red inside. A prism of the proper angle was ground whose dispersion would cancel the first order dispersion of the Cerenkov rays. The rainbow viewed through this prism should coalesce to a narrow band of white light. A picture made through this prism is shown in the illustration also.

The breadth of this last image can be attributed to six effects: 1. Scattering of the proton beam in the material 2. Change of velocity as the material slows the protons down 3. Diffraction effects due to the finite length of proton path in the glass 4. The divergence of the original proton beam 5. Second order chromatic effects 6. The velocity spread of the original proton beam. Estimates of all these effects can be made and graphs of intensity vs. angle for the individual effects and their combined effect are shown in Fig. 2. A micro-photometer record of the Cerenkov image is shown in Fig. 3. If the ordinate of the record is converted to light intensity the agreement is exceptionally good.

The resolution in θ obtainable with the achromatic arrangement opens the possibility of measuring the velocity and hence the kinetic energy of the protons in the beam. Only two factors enter into this measurement -- the angle θ between the proton path and the Cerenkov rays and the index of refraction of the glass. Both of these can be measured with high absolute accuracy and a scale of β and Mev are shown in conjunction with the microphotomer trace.

The instrument used for the energy measurement furnished the pictures of Cerenkov radiation which have just been discussed. The diagramatic layout of the instrument is shown in Fig. 4. The glass in which the Cerenkov radiation is produced is shown in the proton beam. It is a thin sheet of extra dense flint glass (n = 1.88) about 2/3 of a millimeter thick with flat optically polished surfaces. The achromatising prism is shown out of the beam and immediately in front of the Leica camera lens. If the Cerenkov rays were allowed to proceed in their original forward direction the camera would have to be placed directly in the proton beam. To avoid this the surface of the glass sheet through which the beam emerges is aluminized and the Cerenkov rays are reflected back on themselves and emerge in the direction shown. A small projector gives an image of a scale on the film via a small mirror. This scale image is the reference point from which the angle at which the camera sees the Cerenkov radiation is measured. The camera is focussed at infinity.

The problem of relating the position of the image in the camera to the angle θ between the Cerenkov rays and the proton paths is simplified if both directions are measured relative to the normal to the aluminized surface of the glass.

Establishing the direction of the proton beam to within a few minutes of arc is difficult; however this can be avoided by taking two exposures and inverting the equipment between exposures (Fig. 5). A pair of such exposures is shown in Fig. 6. The average of the two positions of the Cerenkov rays will be, very accurately, the position that would have been obtained if the proton beam had been parallel to the axis about which the equipment was inverted. This approximation is better the more nearly the axis of inversion approaches the beam direction.

This inversion is carried out by mounting the instrument assembly of Fig. 4 on a platform whose hollow cylindrical end pieces, through which the beam passes, rest in two vee supports as shown in Fig. 5. The instrument can then be turned in the kinematical bearing thus provided. A latch will hold the equipment in any one of four positions 90 degrees apart.

The angle between the axis of inversion and the normal to the aluminized surface is accurately fixed by the use of precision angle templates. The assembly of Fig. 4 is supported on the platform by pivots which allow the assembly to be turned about an axis through the center of the glass sheet and perpendicular to the plane of the diagram. The platform and the assembly both carry two semicircular bumpers. A triangular steel template can be wedged between the two sets of bumpers and the angular position of the assembly with respect to the platform rigidly fixed.

The template is wedged in from one side and the position of one of the bumpers is adjusted so that the normal to the aluminized surface is parallel to the axis of inversion (Fig. 7). This is determined by viewing the image of a distant light source reflected by the aluminized surface with a telescope equipped with cross hairs. If the normal is parallel to the axis of inversion the position of the image will not change when the instrument is inverted.

If the template is now wedged in from the other direction (Fig. 7 right) the angle between the normal to the mirror and the axis of inversion is exactly twice the angle of the template.

The angle templates were ground by standard precision machining techniques using a sine bar and gauge blocks. The amount of rotation of the assembly has been checked by viewing images of distant objects reflected in a mirror attached to the assembly and then measuring the angular separation of the objects seen in the two positions of the assembly with a surveyor's transit. The rotation was measured as (36° 26.1 ft.) $\pm$ 0.5 ft. The machinists value for the template was (19° 13 ft.) $\pm$ 0.2 ft.

The position of the film image can be related to the angle between the ray directions inside the glass and the normal to the aluminized surface by the following procedure. The camera back is removed and an assembly carrying a cross hair in the plane formerly occupied by the film is substituted. Light from a mercury vapor lamp is sent into the lens from behind the cross hair. An image of the cross hair passes through the lens, through the prism and into the glass sheet where it is finally reflected from the aluminized surface and retraces its path to form a real image in the plane of the cross hair. The light of the 5461 A. mercury green line is used (the achromatising prism serves as a monochromator). The prism is set for minimum deviation and the cross hair is set so that its reflected image coincides with itself. The scale projector is turned on and the central line of the scale is adjusted to coincide with the position of the cross hair and its image.

The relation between the scale divisions on the film and direction as seen by the camera was measured by superimposing the scale on a picture of a distant scene and then measuring the angles between the apparent positions of the lines in the scene with a transit. The separation was found to be 61 ft. Since

the prism is at minimum deviation it does not alter the apparent separation of the scale divisions in the region of the center of the scale. Because of refraction at the surface of the glass the angular separation of the rays inside the glass corresponding to one scale division is 61 ft. divided by the index of refraction (since the rays are nearly normal to the surface and the angles if incidence and refraction equal their sines) or 32.4 ft.

From this it is known that if an image of Cerenkov radiation is formed at the position of the center line of the scale by light of 5461 A, the ray direction inside the glass was normal to the aluminized surface. If the image is not at the center line one can interpolate the angle between the ray and the normal by reference to the scale divisions.

It must be understood that the above discussion has applied to light of 5461 A. If light of another wave length is chosen for discussion the index of refraction of both the prism and the glass sheet will be different. Using the data from this other wave length, a given position on the scale combined with the change in deviation of the prism and the change in refraction at the surface of the glass will give a different Cerenkov angle Θ. Disregarding small second order effects, if the velocity of the proton is calculated using this new Θ combined with the new index of refraction for the glass one obtains the same proton velocity as would have been calculated on the basis of the 5461 A. ray. This is another way of stating the achromatising condition for the design of the prism. The 5461 A. mercury line was chosen for emphasis because it is readily available and its position in the spectrum corresponds to the wave length of minimum second order chromatic deviations for this particular instrument.

The absolute accuracy with which Θ was measured has to be estimated as the sum of errors in a number of procedures indicated above. The estimate of the overall accuracy in Θ is $\pm$ 2.5 ft.

The index of refraction of the glass sheet was known by measuring the index of refraction of a small prism ground from a section of the same piece of raw glass from which the sheet was ground. This measurement was the standard one of prism angle and minimum deviation made on a precision spectrometer table. The results were corrected for the index of refraction of air. The index of refraction for the 5461 A. line relative to vacuum was 1.87957 $\pm$ 0.00034.

Because the width of the Cerenkov image is produced largely by effects thought to be symmetrical, except for the chromatic effects for which correction will be made, it is assumed that the mid point of the image will correspond to the mean energy of the proton beam. The film is read with a microphotometer (the central parts of the scale lines have been left out to leave a clean path for the microphotomer) and the trace width is bisected at several heights and the average mid-point taken. This reduces the effect of random density fluctuations in the film.

The curvature of the Cerenkov image and the problem of relating the microphotometer trace to the scale lines introduces errors in reading the trace. An estimated error in reading the film corresponds to 1.6 ft in Θ.

The estimated errors in the measurement of Θ and n and in reading the film are summarized below along with their equivalents in velocity and kinetic energy.

		$\Delta \beta$	Δ Mev
Error in θ	$\pm$ 2.5 ft.	$\pm$ 0.0004	$\pm$ 0.6
Error in n	$\pm$ 0.00034	$\pm$ 0.00012	$\pm$ 0.2
Error in reading	$\pm$ 1.6 ft in θ	$\pm$ 0.00025	$\pm$ 0.4
Total error		$\pm$ 0.0005	$\pm$ 0.8

The estimates of errors quoted above are admittedly not conservative. However the results are in convenient agreement with experiments which have been performed simultaneously with the use of this equipment.

For instance the range energy relation has been checked by Mather and Segrè in UCRL-1089. The results of their copper ranges are plotted in Fig. 8 along with the predicted range given by Aron, Hoffman, and Williams[3]. The disagreement is of the type and magnitude to be expected. The slope of the predicted range energy curve should be quite accurate and using this it can be seen that the energy measurements are at least consistent (all angle adjustments were remade between runs). The values of the average ionization potential which one obtains from these range energy measurements agree reasonably well with the best previously reported values (for aluminum and beryllium).

In Mather and Segrè the quoted energy error was rounded off to 1 Mev. The errors (largely of a mechanical nature) in the Cerenkov apparatus will be re-evaluated to see if this figure should be enlarged.

Cartwright et al in UCRL-1096 have based a π^+ meson mass determination on energy measurements made with this apparatus. With the setting of the range energy curves by Mather and Segrè it was also possible to derive a meson mass from some previous data of V. Z. Peterson in UCRL-713. Both of these results are in the range of previously accepted values of the meson mass.

A list of the energy measurements made with this apparatus is appended. It corroborates something already known locally from range measurements, that the energy of the deflected beam from the 184 inch cyclotron is remarkably constant once the controls have been set but a complete readjustment of the controls after an intervening duty on other experiments often results in a different energy. This fact is illustrated in Table I.

The use of this instrument is not difficult as no troubles are encountered with background and a satisfactory image can be obtained with a three minute exposure at peak beam intensity (total beam about 10^{-10} amperes, not all of this is effective, and Kodak Lineagraph Pan film). However, a beam of small divergence is necessary and the exposure becomes uneconomically long for greatly reduced intensities. A range measurement is probably of more universal applicability and has the advantage of greater intrinsic reproducibility. The range measurement may be converted to energy with only slightly less accuracy using the results of Mather and Segrè.

[1] P. Cerenkov, Phys. Rev., 52, 378 (1937);
Collins and Reiling, P.R. 54, 499 (1938);
Wyckoff and Henderson, P.R. 64, 1 (1943).
[2] I. Tamm, Journal of Physics, USSR 1, 439 (1939).
[3] Aron, Hoffman, and Williams, AECU-663 (UCRL-121).

TABLE I

Mean Energy of the Electrically Deflected Proton Beam from the
184-inch Cyclotron as it Enters the Cave. (Rest Energy of the
Proton Taken as 938.17 Mev.)

Date	Energy	Associated Experiment
9/13/50	339.0 338.5	Range (Segrè)
9/25/50	341.2 341.3 341.5 341.3	π^+ meson production (Cartwright)
10/9/50	339.7 339.4 339.3 339.2	Range (Segrè)
12/24/50	340.5 340.6 340.5	Range (Segrè)

UCRL-1191

WITHOUT PRISM

θ (DEGREES)

36 37 38 39 40 41 42

WITH PRISM

Fig. 1

1. SCATTERING   2. SLOWING   3. DIFFRACTION

4. DIVERGENCE   5. CHROMATIC EFFECTS   6. ENERGY SPREAD

ALL SIX EFFECTS COMBINED
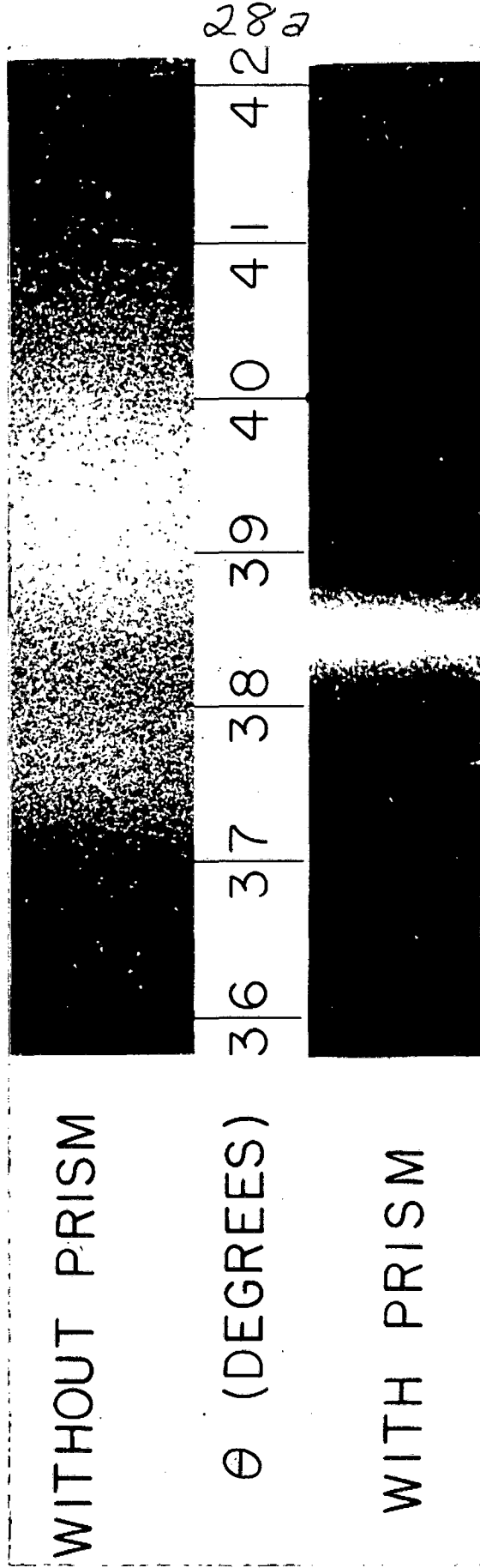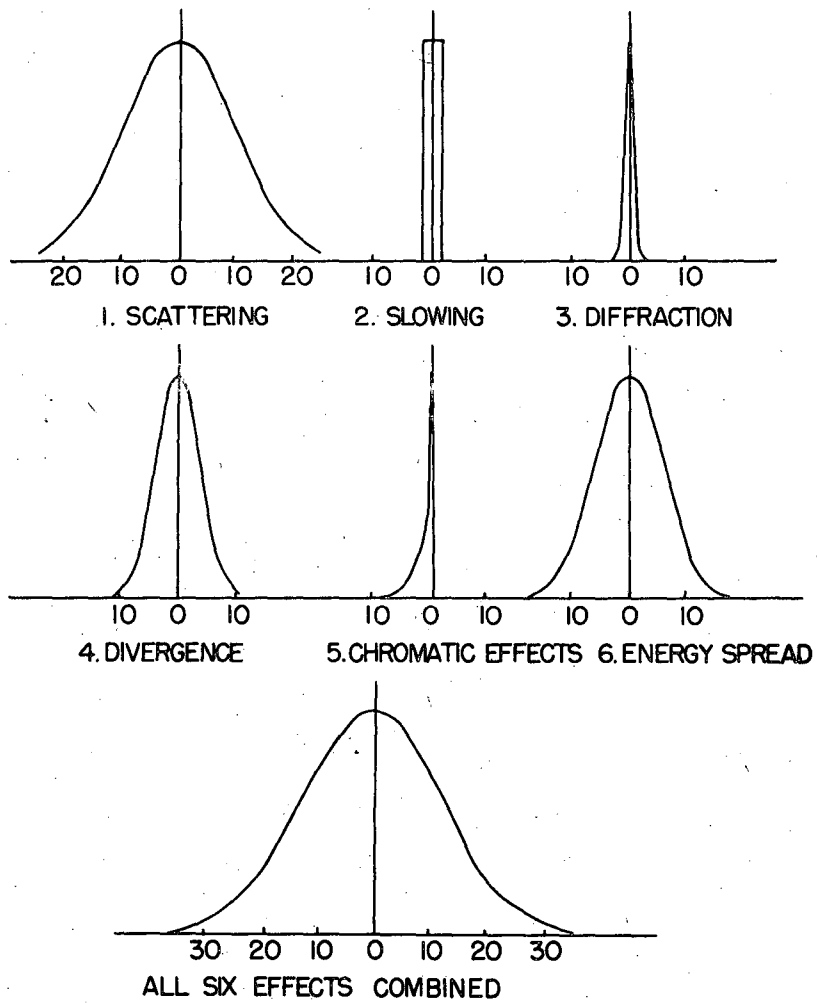
ESTIMATED   ANGULAR   INTENSITY   DISTRIBUTION   OF THE
ACHROMATIZED   CERENKOV   RAYS   (IN EQUIVALENT MINUTES
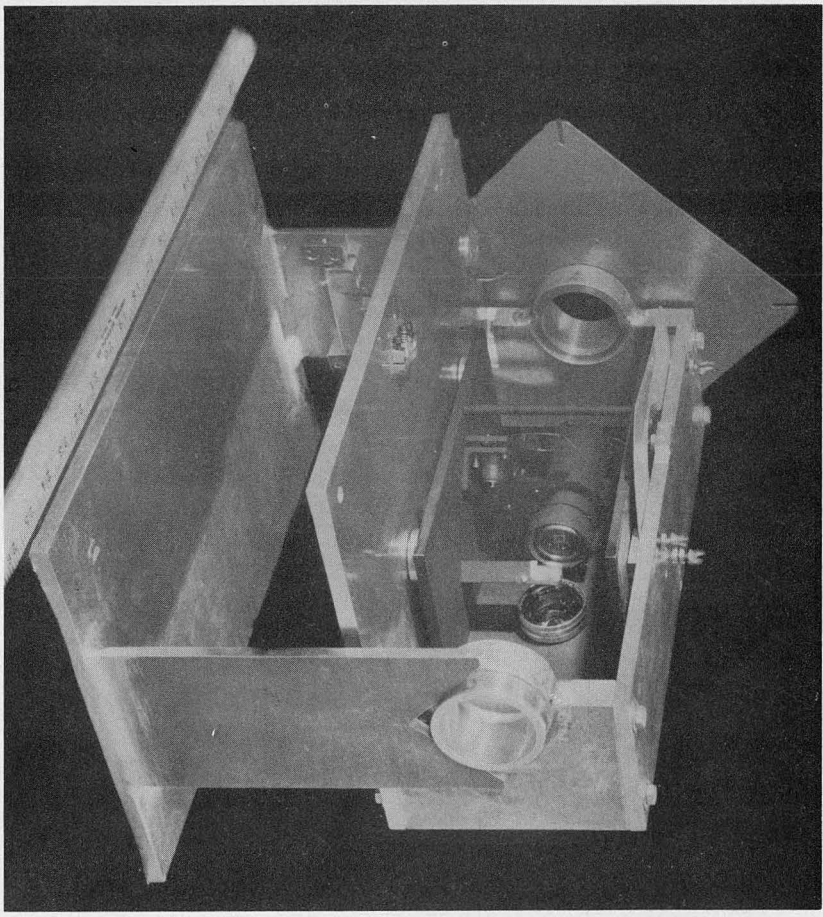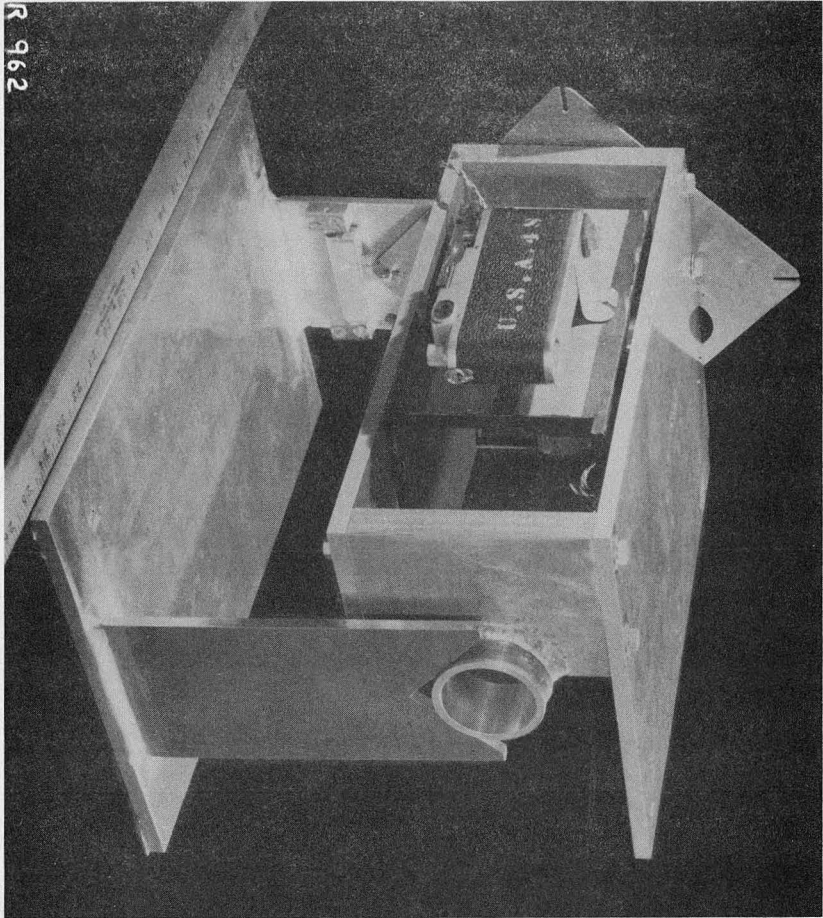OF ARC IN θ)

FIG.   2   MU 1422

Fig. 3

Fig. 4

Fig, 5
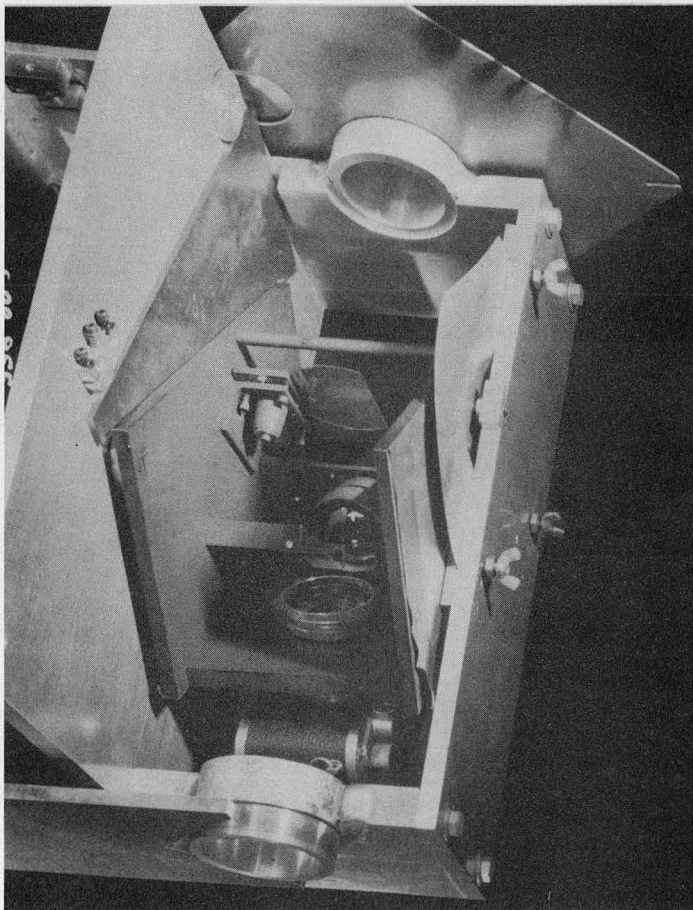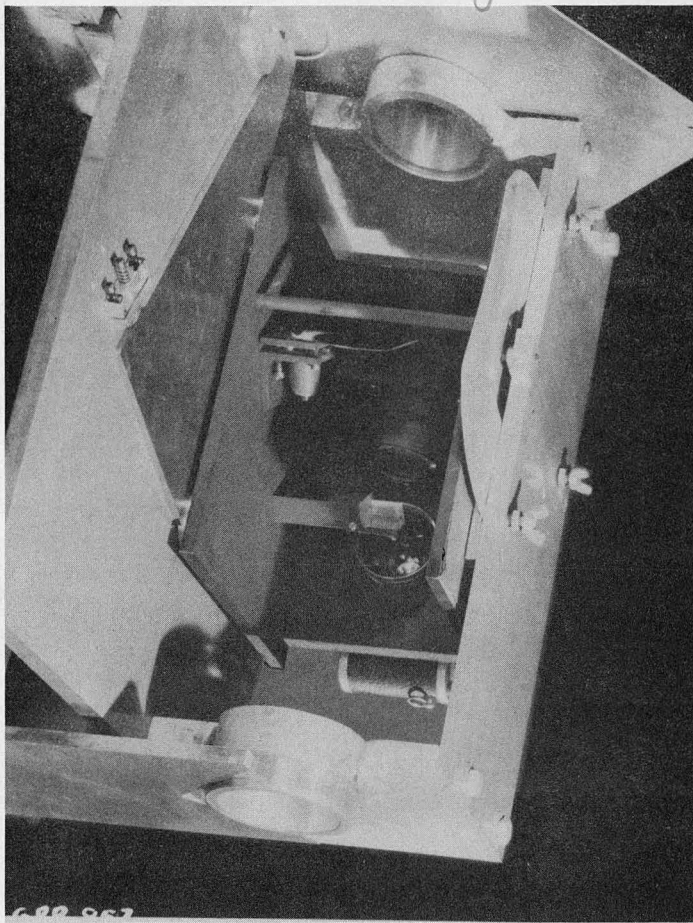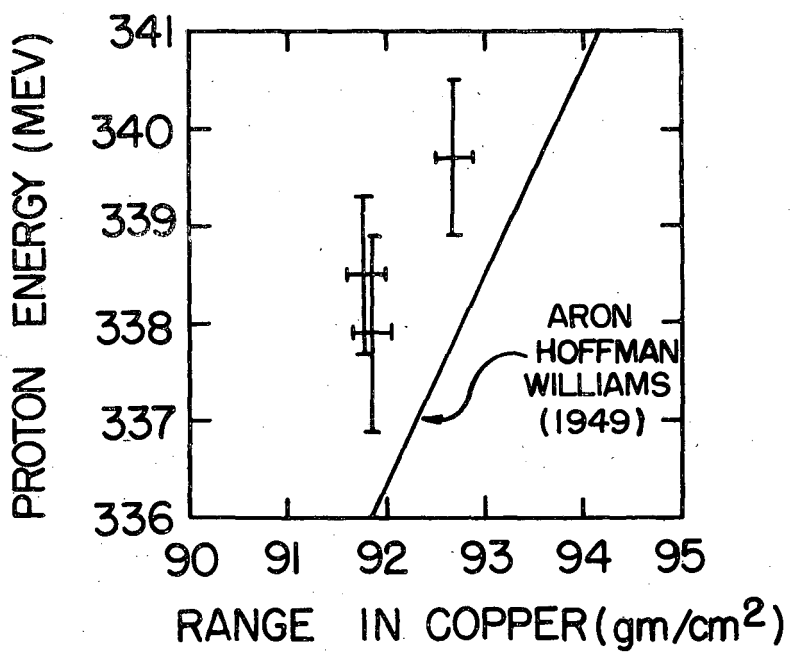
ZN-37

ZN-38

Fig. 6

ZN-38
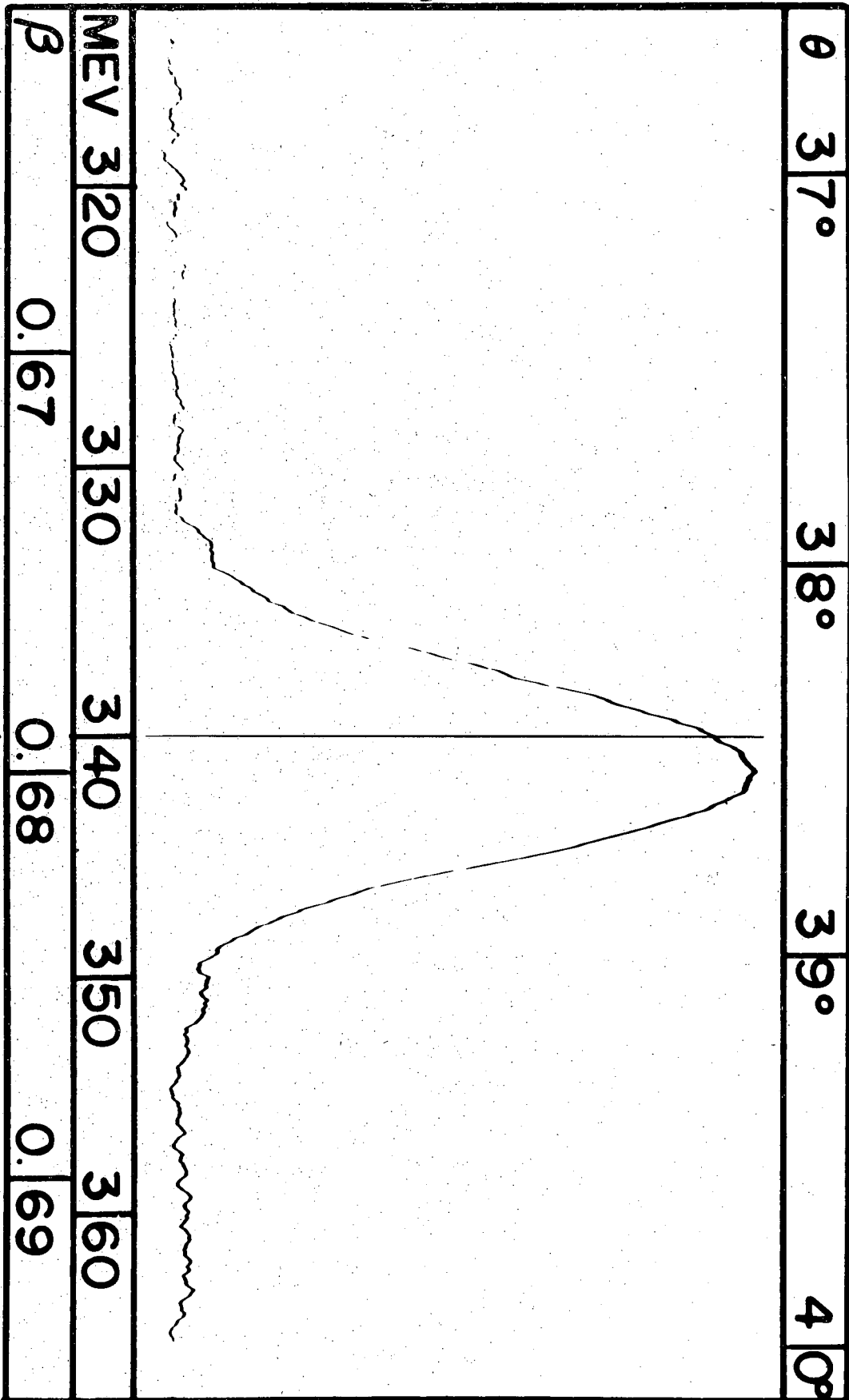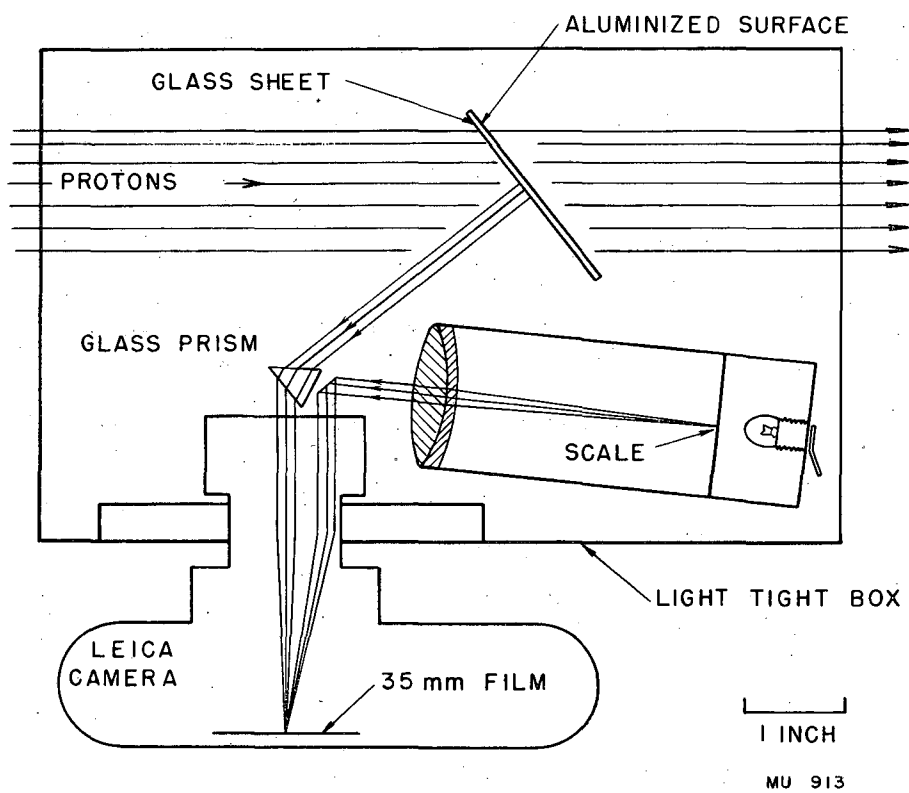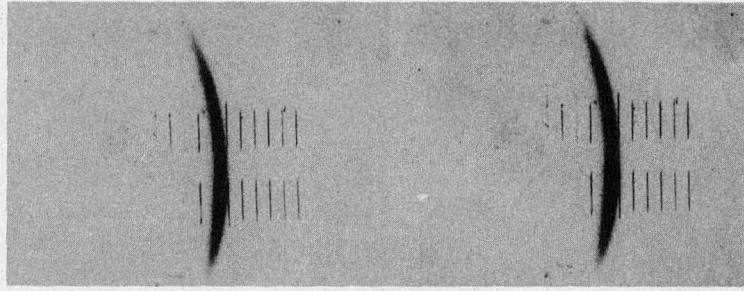
Fig. 7

FIG. 8

MU 1423

5. Delayed Neutron Emitter

William Gardner

More data on the delayed neutron activity of 0.177 second has been obtained. The relative yields/atom have been compared for the elements which produce this activity --notably Be, B, C, and N. This and the ratio of yield between boron and beryllium for protrons and deuterons indicate that the parent nucleus is quite likely Li^9.

Quite recently the beta energy distribution for the above radioactivity has been observed with the employment of a Sprial Orbit Beta Ray Spectrometer. This is used in the external cyclotron beam in conjunction with neutron counters so that the neutron beta coincidence may serve as a check. First results indicate an E_{max} of the beta of about 10 Mev which is in agreement with previous mass calculations of Li^9.

6. The Neutral Meson Program on the 184-inch Cyclotron.

Walter Crandall, Richard Hales, R. H. Hildebrand, Norman Knable, Richard Madey and B. J. Moyer

During the past quarterly period two major lines of effort have been pursued in the neutral meson program: first, the construction of improved equipment for measurement of the angular correlation and distribution of photon pairs from π^0 decay; and second, the development of a new type of photon detector to detect π^0 decay with relatively high efficiency for use in cross section measurements.

Photon Pair Detector. The success of the improved electronics described in the last report UCRL-1057 made it worthwhile to construct equipment for more accurate and convenient alignment of the scintillation counter telescopes. A further refinement of the equipment was the development of magnetic shields for the phototubes. This shielding is necessary because the stray field of the cyclotron is about 30 gauss in the region where the experiments are conducted and this is enough to cause large changes in the sensitivity of unshielded phototubes when they are moved to make measurements at different angles.

The telescope supporting yoke and magnetic shields are now almost ready for use.

New Type Photon Detector. This type of detector which was briefly described in the last report UCRL-1057, is shown in Fig. 1. Photons from π^0 decay in the target strike a converter in which electron pairs are formed and then scattered through wide enough angles to be detected in adjacent counters.

In the idealized arrangements of Fig. 2, half of the electron pairs formed would be scattered in such a way that one electron enters each counter. Thus the efficiency would be independent of the scattering angle and should depend on the quantity

$$\frac{\rho x}{A} \cdot Z^2$$

where ρ is the density, x the thickness, A the atomic weight and Z the atomic number of the converter used. The efficiency of the actual arrangement used (Fig. 1) varied very nearly in this manner. Thus the predicted and measured relative efficiencies of thin Pb, Cu, Al, and C radiators are given in Table I.

TABLE I

	Pb	Cu	Al	C
$\dfrac{\rho x}{A} Z^2$	1	.309	.12	.05
Observed relative efficiency	1	.307±.050	.08±.04	-.04±.05

As a further check on the apparatus Pb converters of various thicknesses from 1/16 inch to 5/16 inch were used and the efficiency was found to change as expected for photons whose energy distribution is that resulting from π^0 decay. A third check of the equipment consisted in demonstrating that the counting rate varied linearly with target thickness. When the target is removed completely the counting rate drops to about 2 percent of the count with target and converter in.

The counting rate with the target and converter in place is about 4-1/2 times the rate obtained with the converter removed. This converter-out background is not yet thoroughly understood. It disappears when the counters are moved far apart and is relatively higher for Al than for C targets. The next experiments with this detector will be made with a counter ahead of the radiator to determine whether the background is due to correlated charged particles from the target.

The results on yield from hydrogen thus far obtained with this detector are given in Table II.

TABLE II

Relative Differential Cross Sections for Producing Photons
at (120°)

σ_H	-0.020 ± 0.032
σ_C	1.000
σ_{Al}	1.67 ± 0.17

The hydrogen cross section is obtained from carbon and polyethylene target differences. It will be noticed that the hydrogen cross section is low in agreement with former pair spectrometer results.

Some success has recently been obtained in eliminating counters C and D (Fig. 1) and substituting a fast bridge type double coincidence circuit in place of the quadruple circuit.

This has the advantage of reducing the equipment necessary for each detector and may allow the operation of apparatus such as that schematically shown in Fig. 3. Each pair of counters is an electron pair detector. The output of each fast coincidence circuit is fed into a slow coincidence unit which records coincidences between photon pairs. This would allow rapid angular correlation and absolute cross section measurements with a minimum of equipment.
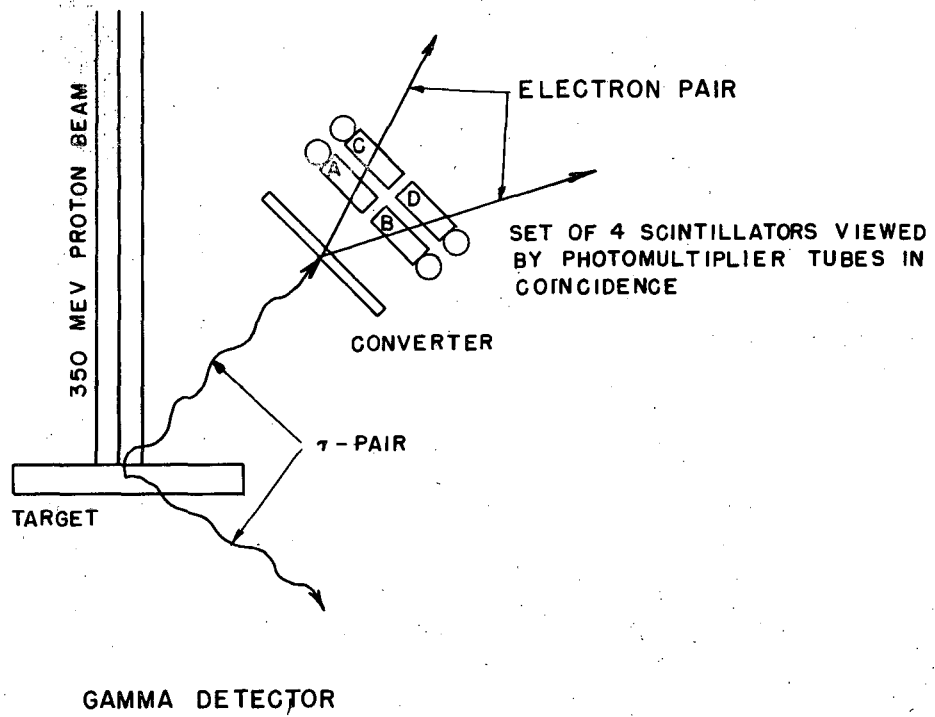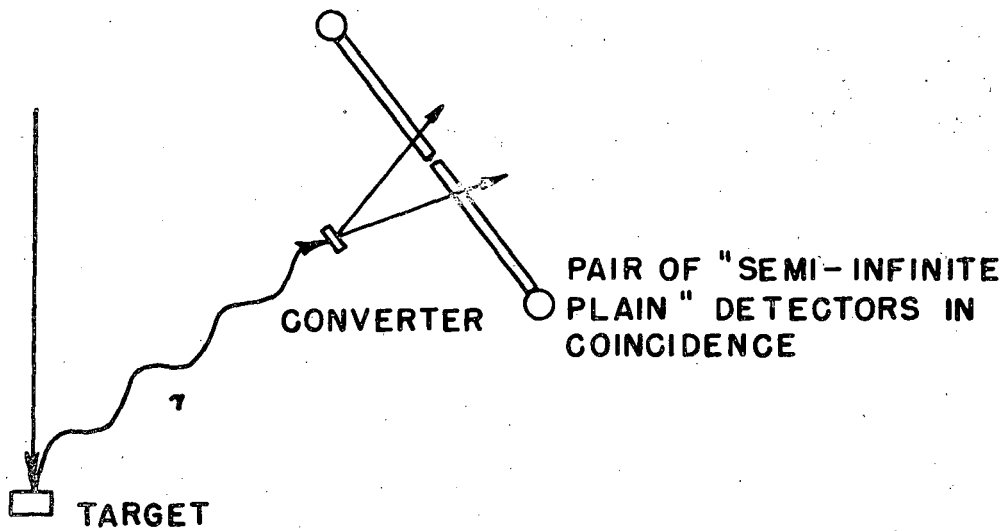
ELECTRON PAIR

SET OF 4 SCINTILLATORS VIEWED
BY PHOTOMULTIPLIER TUBES IN
COINCIDENCE

CONVERTER

350 MEV PROTON BEAM

γ - PAIR

TARGET

GAMMA DETECTOR

FIG. 1

MU 1654

CONVERTER

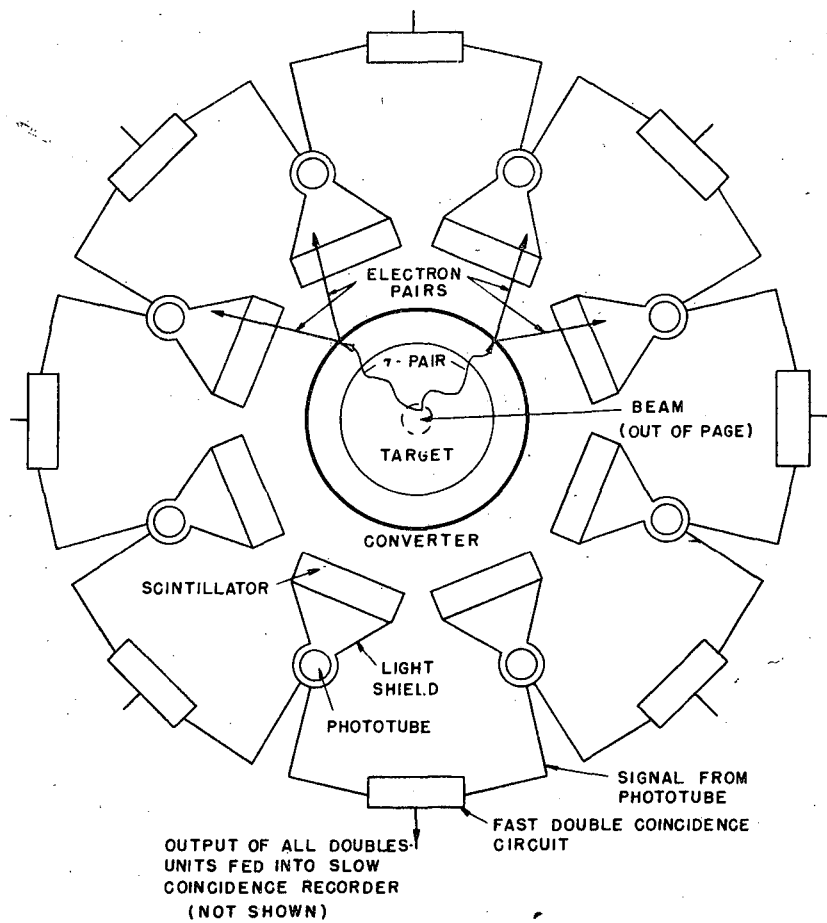PAIR OF "SEMI-INFINITE PLAIN" DETECTORS IN COINCIDENCE

TARGET

IDEALIZED GAMMA DETECTOR

FIG. 2

SCHEMATIC DRAWING OF PROPOSED MULTI-UNIT γ-PAIR DETECTOR

FIG. 3

MU 1658

7. π Meson Detection

L. Neher, and J. Carothers

Experiments have been undertaken to count π mesons produced at the synchrotron using a time of flight method. The mesons were produced in a target placed in a magnetic field, which allowed separation of the positive and negative particles. Channeling selected a definite momentum interval, and the velocities of the particles fitting channel were measured. High energy β particles gave a counting peak at a β of one. There is another counting peak in the velocity region corresponding to that of a π meson fitting the momentum channel. A reduction in beam energy below the meson production threshold eliminates these counts. Range curves are being run, but owing to the low counting rate (15-20 counts per hour) these are not yet conclusive and the identification of the particles is consequently tentative.

8. Electronic Detection of Positive and Negative Photo Mesons

J. Carothers, and L. Neher

An experiment has been started attempting to separate positive and negative mesons produced by the synchrotron beam. The 350 Mev pair spectrometer is being used to achieve the resolution. The mesons are being detected by a combination of counter telescopes and a time of flight detection method. This was found to be necessary in order to discriminate against a large number of secondary electrons and positrons. Satisfactory preliminary results have been obtained which indicate counting rates of the order of 3/minute for positive and negative mesons are reasonable for light elements as primary targets. The main purpose of these experiments is to obtain reliable +/- ratio measurements independent of visual uncertainties.

9. An Experiment to Determine the Spin of the Positive π Meson

K. Crowe, F. Crawford, M. L. Stevenson

Following the suggestion by Professor Robert E. Marshak of the University of Rochester, an experiment has been started to determine the spin of the π^+ meson in a manner which is independent of any detailed caluclations beyond general quantum mechanics principles. The experiment consists of measuring the absolute cross section of the process: $\pi^+ + d \longrightarrow p + p$. This is the inverse process of the reactions recently measured by Cartwright, Peterson, Richman and Whitehead. If one applies the principle of detailed balance to this process and its inverse, then the ratio of the cross section depends directly on the statistical weights of the respective final states. Accordingly, the spin values follow directly. The experiment consists of bombarding a heavy water target in the positive meson beam, as recently described by Richman, Skinner, Whitehead and Youtz. An arrangement of scintillation counters serves to identify the mesons. The resultant 70 Mev protons are detected in a pair of NaI crystals in coincidence. A preliminary run has shown that this experiment is feasible.

10. Meson Experiments

C. Richman, M. Skinner, W. F. Cartwright and M. Whitehead

<u>Scattering of π^+ Mesons by Carbon</u>. The experiment on the scattering of π^+ mesons by carbon has yielded a result for the differential scattering cross section of 90° of $(2.2 \pm 1.0) 10^{-26}$ cm^2 steradian^{-1}. The experimental arrangement used to obtain this result differed from that used in the original attempt to detect scattered mesons by nuclear emulsions. All improvement in the geometry made it possible to place the plates much closer to the carbon scattering target, thus improving the detection efficiency.

<u>π^+ Production by P-P Interaction at 0°</u>. The π^+ production by p-p interaction at 0° has yielded as an incidental result of the cross section determination, a value of the π^+ meson mass of 275.1 ± 2.5 electron masses. At the same time the shape of the meson spectrum indicates that the intense peak at maximum meson energy corresponds to the reaction $p + p \rightarrow \pi^+ + d$. The cross section for the reaction $p + p \rightarrow \pi^+ + d$ is determined to be $(1.30 \pm 0.26)10^{-28}$ cm^2 ster^{-1}. The cross section obtained by integrating the <u>entire</u> spectrum is $(2.0 \pm 0.4)10^{-28}$cm^{2}ster^{-1}.

<u>π^+ Production by P-P Interaction at 60°</u>. The π^+ production by p-p interaction at 60° (Lab System) has yielded a value for the total production cross section at 60° of $(0.08 \pm 0.04)10^{-28}$ cm^2 ster^{-1}. This datum, together with the results at zero degrees indicates that the angular distribution of mesons in the center of mass system is $(0.06 ^{+0.07}_{-0.05} + \cos^2 \theta)$.

π^- Mesons. The pulse height detection method, as mentioned in UCRL-1168, is now being employed to count negative mesons produced by the external proton beam of the synchrocyclotron. The production of π^- mesons as a function of the target Z will be investigated in the near future.

11. π-Meson Production Cross Sections in Helium (synchrotron beam)

M. Jakobson, A. Schulz and R. S. White

The energy distribution of π^+ mesons produced by synchrotron photons on helium has been measured for three angles -- 45°, 90°, and 135°. The π^+ mesons were detected electronically by π^+ decay, by μ^+ decay, and by both decays in coincidence. Emulsions were exposed at the same time from which the π^- production should be obtainable.

12. Effect of Chemical Binding on Stopping Power

T. J. Thompson

Relative stopping powers of various substances will be measured with the 345 Mev proton beam from the 184-inch cyclotron. An accuracy of about 0.1 percent will be attempted. Various carbon and hydrogen compounds will be studied

first, because of their availability in a great variety of chemical forms.
A preliminary run has been made. No data considered trustworthy are on hand at
this time.

13. Measurements of Fission Cross Sections with Charged Particles.

T. J. Thompson

The short duty cycle of the modern pulsed machines has made it difficult
to detect fission while the primary beam is passing through the ionization
chamber. An arrangement of two ionization chambers, in which the fission sample
is present in one only and the other is used to obtain a pulse from the primary
beam which may be used to cancel the effect of the beam in the first chamber,
has been built and tested. It shows promise of being able to measure fission
cross sections in the cyclotron beam.

14. Deuteron-proton Scattering using 190 Mev Deuterons.

A. Bloom and M. O. Stern

Measurements of the elastic scattering cross sections are virtually com-
plete. They indicate surprisingly close agreement with the predictions of Chew[1]
in the range of angles 40 to 100 degrees in the center of mass system. From 100
degrees to 140 degrees they show a cross section about half that of Chew,
indicating that the pick-up process is slightly less important than Chew had
expected. Some further effort will be made to extend slightly the range of
angles of the measurements.

Preliminary measurements of the inelastic scattering cross section indi-
cate a close correlation between the angles of the two out-going protons in
the laboratory system. This result was at first surprising, but a closer look
at the energy-momentum conservation relations has shown that the results should
not be unexpected in this case of a deuteron beam incident on a hydrogenous
target. Measurements are not at this time sufficiently extensive to allow
determination of the absolute inelastic scattering cross section. This work
is continuing.

---

[1] Chew, J., Phys. Rev. 74, 809 (1948).

15. Proton-proton Scattering at 120 to 345 Mev

O. Chamberlain, E. Segre and C. Wiegand

A report to be numbered UCRL-1109 is still in preparation, being delayed at this time only by some recalculations of theoretical results. The necessity for such recalculations was not apparent until the report was assembled in fairly finished form.

The experimental results are summarized in Table I.

The results at reduced energies have been reported previously. They cover a much more limited range of angles, all near 90 degrees in the center of mass system. It is planned to continue the work at reduced energies to include small angles from the beam, though it is expected that a new liquid hydrogen target will be needed for this work, and so the results will not be available for some time.

TABLE I

Angle Θ c.m. system in degrees	Differential cross section c.m. system in 10^{-27} cm^2/sterad.	Error (Standard Deviation) in diff. cross section in 10^{-27} cm^2/sterad.	Energy in Mev
Using a liquid hydrogen target:			
11.3	5.2	0.5	345
15	3.5	0.3	
21	3.3	0.3	
33	3.5	0.2	
43	3.4	0.2	
53	3.3	0.2	
Using a CH$_2$ target:			
36	4.1	0.3	
44	4.0	0.3	
46	3.8	0.2	
52	3.8	0.2	
61	3.8	0.3	
64	3.6	0.3	
71	3.7	0.2	
80	4.0	0.3	
88	3.7	0.2	

16. Polarization in Elementary Particle Scattering (Experimental)

L. F. Wouters

Equipment for examining polarization effects in elementary particle scattering has been assembled and tested; data collection an minor modifications are now being carried through.

Polarization here signifies the azimuthal dependence of differential cross section for a beam of particles having a preferential spin orientation. The normal to the plane of an elastic scattering establishes an azimuthal direction with respect to which such a polarized beam would scatter asymmetrically in such an experiment. The magnitude of this asymmetry depends on the force model used in computing the interaction; confirmation of its existence would verify the tensor or non-central nature of fundamental interactions.

From the experimental standpoint no azimuthal effect is observed in a single scattering however, since the interacting particles are intially randomly oriented (i.e., 50 percent spins up, 50 percent spins down). An equal number of particles emerge at all azimuths for a given scattering angle, but there exists a preferential spin orientation at each azimuth.

If a beam of elastically scattered particles is observed at a moderate scattering angle, say $30°$, and is allowed to scatter a second time (elastically), the counting rate in the experiment should now show the azimuthal asymmetry. See Fig. 1. A phenomenological analogy appears in the observation of polarization of light by double reflection (Malus' experiment).

Theoretical aspects of this problem are being considered by Mr. Swanson of the theoretical group; the angular dependence of particle flux intensity for n-n-n scattering in the 250 Mev region is predicted to have the approximate shapes (for a non-central or tensor force model) shown in Figs. 2 and 3.

It is expected that the asymmetry property becomes more evident at higher energies.

The experiment thus consists of elastically scattering a fundamental particle (neutron or proton) twice against similar particles. The two fundamental experiments are illustrated in Figs. 4 and 5.

Considerations of available particle flux intensities, accental background and other instrumental factors show that p-p-p is feasible but would require fairly extensive mechanical changes in the beam deflection system associated with the 184-inch cyclotron. n-n-n is nearly impossible as shown; however, theoretical arguments show that the experiment shown in Fig. 6 would be equivalent. This is quite feasible to perform with the accelerator as presently equipped. The first scattering is performed inside the cyclotron tank using a target located so that the existing neutron beam collimator selects neutrons emergent at an optimum polarizing angle.

For such an experiment the neutron involved in the first scattering should be ostensibly free; the best approximation to such a free neutron target is deuterium. Fortunately a LiD target of adequate size is available for the experiment. The second scattering is performed by the orthodox carbon-paraffin
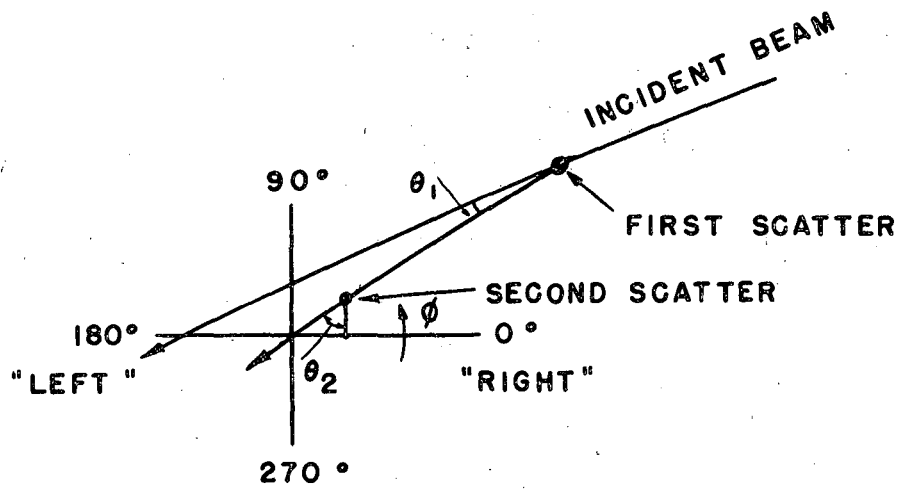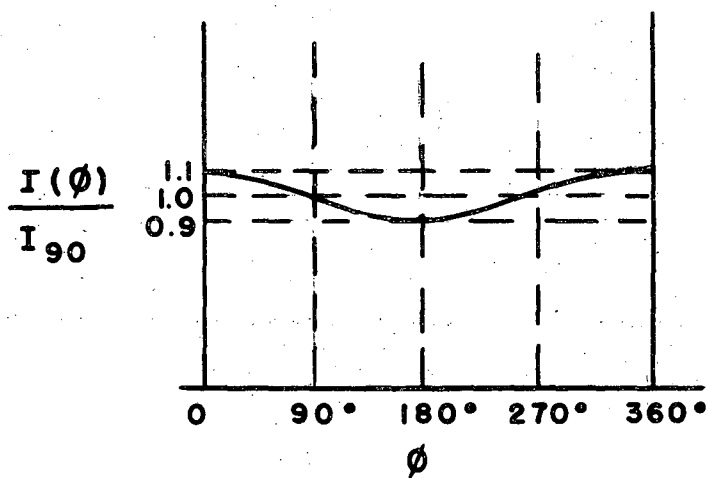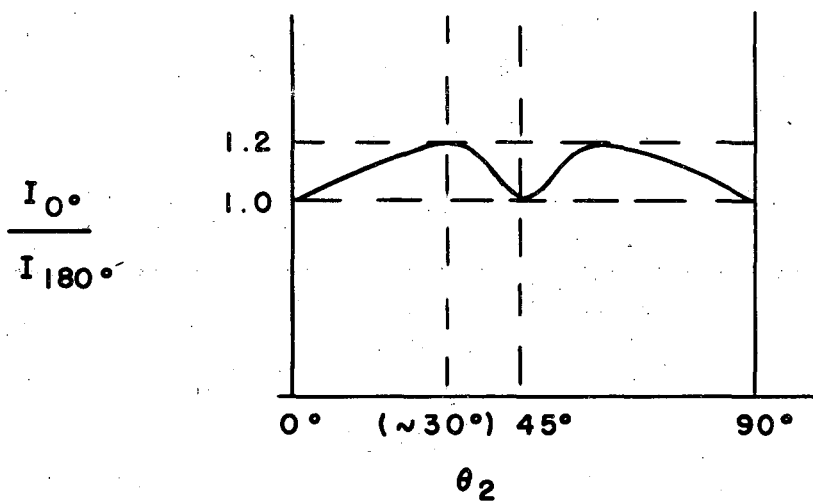
FIG. 1

MU 1655

$$\frac{I(\emptyset)}{I_{90}}$$

FIG. 2

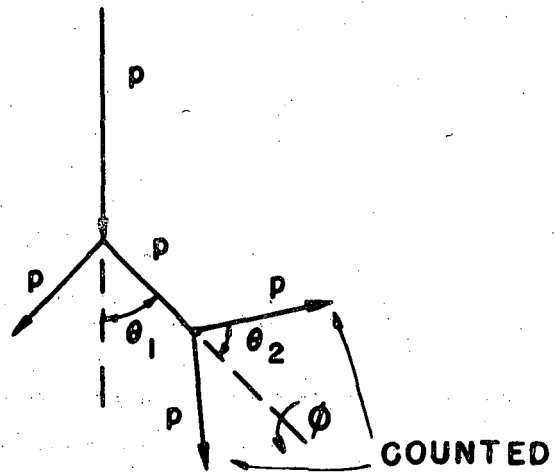$\frac{I(\emptyset)}{I_{90}}$ MEASURED AT OPTINUM SCATTERING ANGLE ($\sim 30°$)

MU 1656

"RIGHT-to-LEFT" RATIO
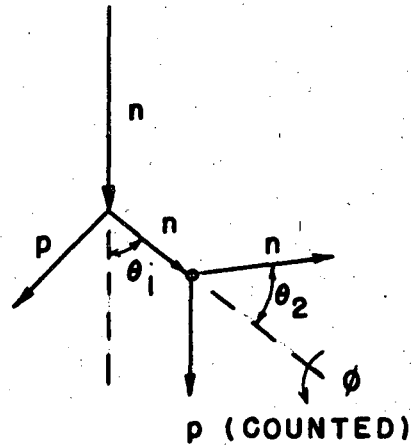
FIG. 3

MU 1659

" p – p – p "

(MEASURES p – p INTERACTION)
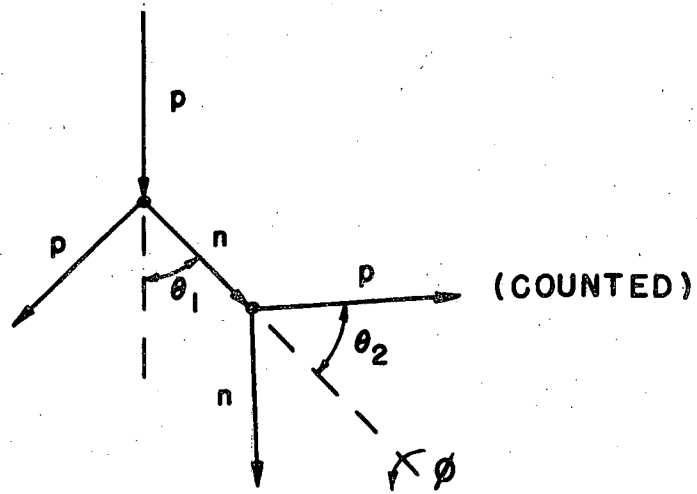
FIG. 4

MU 1660

" n – n – n "

(ACTUALLY MEASURES n– p INTERACTION)

FIG. 5

MU 1661

" p — n — p "

(MEASURES n - p INTERACTION)

FIG. 6

MU 1662

difference method.

The associated counting equipment consists in brief of four sets of
coincidence counter telescopes mounted on an azimuthally rotatable frame; the
scattering angle of the individual telescopes can also be adjusted. The
counter solid angles are purposely made quite large in order to obtain
statistically significant numbers in a finite amount of time. This is permis-
sible, since the polarization effect is only broadly dependent on angles.
Each telescope consists of two liquid phosphor scintillation counters; the
photomultipliers are operated using the pulsed high voltage technique described
in previous reports. The signal circuits consist of four corresponding biased-
diode coincidence units each operating a scaler through a pulse-generating
amplifier. A fifth complete channel is used with a similar telescope employed
as a beam monitor (having its own scatterer). The resolution time of these
systems is about 0.005 microseconds; no difficulty is encountered in establish-
ing reasonably good proton plateaus with complete counting linearity up to the
highest available fluxes.

A comprehensive report describing the design and technique of scintilla-
tion counting in this energy region is in preparation.

17. Synchrotron Studies

A. C. Helmholz

During the months of November, December, and January the synchrotron
was out of operation for about three weeks due to vacuum leaks in the rubber
gaskets between quartz sections of the donut. During the remainder of the
period, the operation was good and considerable experimental work was accomp-
lished.

Neutron Yields. The work on neutron yields by W. Jarmie, L. Jones, and K.
Terwilliger has been completed and has been submitted to the Physical Review
for publication. The work essentially confirms that of Kerst and Price, and
finds that the yield per atom increases as $Z^{1.7}$ instead of Z^2. More data has
been obtained at low Z, where the neutron yield seems to depend on the binding
energy of the neutron. This is to be expected since the "effective" number of
photons increases with energy.

Angular Distribution of Shower Gamma-Rays. The work of J.Rose on angular distrib-
ution of shower gamma-rays has also been completed and has been submitted to
the Physical Review for publication. The angular distribution of gamma-rays
(of about 17.5 Mev as detected by Cu foils) agrees fairly well with the theory
of S. Fernbach and L. Eyges.

Measurements with the Pair Spectrometer. During this period the pair spectro-
meter has been put into operation. So far only one liquid scintillation counter
for positrons and one for electrons are in use, but these are operating success-
fully. Preliminary measurements of some Y-ray absorption coefficients have
been made. The pair spectrometer magnet is also being used by L. Neher and

J. Carothers for the measurement of yields of π^+ and π^- mesons. In this experiment the mesons are formed in the middle of the magnet, are selected in momentum by their curvature in the field, and their time of flight outside the magnetic field is measured. This (the momentum and velocity) provides a measurement of the particle mass. The main contamination, of course, is electrons.

π^+ Meson Yields. A rather large amount of running time was consumed by the experiments of R. S. White and M. Jakobson on the yield of π^+ mesons from K, D, and He. They employed the high pressure target designed by White, and measured the π^+ mesons by means of coincidences in two crystals, plus the delayed coincidence due to the μ meson from the $\pi \rightarrow \mu$ decay. In addition, nuclear emulsions were exposed, which will give information about the π^- mesons, and the π^+ at small angles (45°) where the counter backgrounds are so large as to make the counting impossible. The experiments were conducted with H_2, D_2, and He alternately as the target, each gas being run several times. The data on yields vs. energy at 90° and 135° for each substance are being analyzed at present. Particularly the data on the comparative yield from H and D should be interesting for some fairly simple theoretical arguments can be made concerning the ratio.

Li^8 Production by γ-Ray Bombardments. F. Coensgen is investigating the yield of Li^8 produced by γ-rays bombarding different elements. He has found an additional short life activity with half-life of the order of 2 sec. This may be the Li^9 activity reported by others in this laboratory.

Other Studies. The work of R. D. Miller on photo-produced stars has continued. A preliminary report has been submitted to the Physical Review for publication as a letter. Work on electron electron scattering by W. Barkas, C. Violet, and F. Gilbert has used some synchrotron time. They employ the pair spectrometer to select definite energy electrons or positrons, whose tracks in photographic emulsions are examined.

18. Theoretical Physics

K. Watson

The analysis of the high energy transmission of neutrons through complex nuclei has been interpreted as implying that n-n and p-p scattering are similar at high energies.

A re-evaluation of the theoretical range energy relations has been made on the basis of the technique recently developed here to measure proton energies by means of their Cerenkov radiation.

Further work has been completed in analyzing the moments of the angular distribution of electrons and photons in a cosmic ray shower.

A study of the relation of the γ-ray spectrum resulting from the absorption of π^- mesons in deuterium to the n-n force has been completed.

II ACCELERATOR OPERATION AND DEVELOPMENT

1. 184-inch Cyclotron

J. Vale

Operation. Operation of the 184-inch cyclotron was very good during this period, with an average operation of about 95.6 percent. The last two months each averaged about 97.5 percent. The first month, about 92 percent. The lower figure was caused by a shutdown that was necessary in order to install concrete blocks in the main shielding.

Main Concrete Shielding. The additional concrete shielding is now about 95 percent completed. The only remaining blocks that have not yet been installed are the triangular shaped ones that fit into the corners. These blocks serve to thicken the shielding at the corners so that there will be at least fifteen feet of concrete at these points.

The additional wall on the south-east side was spaced about five feet from the then existing shielding. This provides an enclosed area that can be used for the storage of radioactive substances, including radium test sources.

During the past several months, emphasis on the cyclotron has been placed on steady operation rather than development of the machine. This has been necessitated primarily by the shortage of manpower.

2. 60-inch Cyclotron

G. Bernard Rossi

Bombardments were performed during this period consuming 1228.5 hours of the available 1513.2 hours. Alphas, deuterons, protons and C^{+6} ions were used in the bombardments in the following proportions:

Alpha bombardments	561.9 hours
Deuteron bombardments	401.0 hours
Proton bombardments	35.1 hours
Carbon bombardments	186.4 hours
Experimental operation	44.1 hours
Total Bombardment Time	1228.5 hours
Operational Outage	284.7 hours
Total Available Time	1513.2 hours
Shutdown	494.0 hours
Holidays	182.5 hours
CO_2 installation	18.3 hours
	694.8 hours
Total Time	2208.0 hours

During the period, therefore, the cyclotron was in productive operation for 81.2 percent of the available time. It will be noted that 18.3 hours were spend installing a CO_2 system. This is a gas controlled rate of rise fire protection system which will discharge six large (50#) CO_2 cylinders into the room containing the cyclotron. These cylinders discharge after one minute of siren warning to allow the area to be cleared of personnel. In addition, six more cylinders may be discharged mechanically through the same system if necessary.

An oil tight sill has been installed around the periphery of the room to create a reservoir to contain the magnet cooling oil in the event the tanks rupture. Thus, an oil fire would be isolated to the room containing the discharge system.

3. Synchrotron

George C. McFarland

During the month of November an automatic liquid nitrogen dispensing system was installed. This system for keeping the synchrotron traps cold is quite simple in design and has proved itself highly efficient. A high intensity beam was available throughout the month. Some long bombardments were scheduled, including one continuous use of the beam over a sixty-four hour interval.

Several times during the month the beam energy was reduced to 250 Mev in the course of experiments. This was easily accomplished by reducing the magnet excitation. There was no loss in intensity at 250 Mev. In addition, other reductions in energy down to 150 Mev were accomplished readily by shortening the rf pulse length.

Some preliminary tests were made on the synchrotron with devices designed to improve the reliability of operation and increase the beam intensity. These tests were performed during breaks in the experimental program or after the regular shift. They indicated that certain refinements and debugging must be accomplished before their full value is realized. The devices tested were the capacitor H.V. servo-regulator which showed tendencies to oscillate, the beam intensity servo-regulator, and a contractor as suggested by J. Lawson of General Electric Company.

Early in December, operation was interrupted because of poor vacuum caused by deterioration of the rubber segment joining gaskets. The machine was disassembled and the vacuum chamber reworked. Considerable difficulty was encountered in reassembly due to partial deterioration or flaws in the spare gaskets which had been stored on a shelf in the machine room.

About the twentieth of December, the machine was back in operation but somewhat erratic and below average in beam intensity. Experiments continued during this time.

Early in January operation returned to normal. The synchrotron continued to perform reliably and at high intensity levels during the remainder of the month.

4. Linear Accelerator and Van de Graaff Machines

W. K. H. Panofsky

At this writing the physical changes made in the linear accelerator and electrostatic generator plant are completed and the machine has yielded a satisfactory beam. Accordingly we summarize here the physical changes made in the last 8 months.

The Van de Graaff was partially reconstructed, that is, new textolite supports were installed in the upper section and the high voltage end was completely re-wired with new power units being installed in most cases. Extensive precautions were taken to avoid freon corrosion. The Van de Graaff was made movable so that it is possible to operate in two positions, 13 feet apart, or any chosen spot in between. The purpose of this arrangment is to permit a large bunching distance. These changes can be effected in a maximum time of two hours. New oscillators were installed on the linear accelerator, only 9 now being necessary to replace the original 25. Pulse transformers were installed to provide the higher plate voltage required. The counting area has been completely remade with 6 new racks and many new pieces of equipment installed. In the past several weeks operational tests have been made on the completed accelerator and results are as follows. The Van de Graaff machine shows marked improvement with no trouble being experienced in two weeks of operation. It was found possible with the new ion pulser unit to obtain a total peak current of 4 milliamperes, as compared to the previous 2-1/2 - 3 milliamperes. No difficulty has been encountered in obtaining the 4 Mev injection voltage. It has also been found that the physical position of the Van de Graaff can be maintained within 1/16 in. while moving from one extremity of travel to the other.

Although it is somewhat early to predict the ultimate operation of the new oscillators, present observations show that they are many times more reliable than the former Baker type oscillators. Evidence would indicate that most of the oscillator troubles encountered so far have been the result of vacuum tank sparking. It is hoped that this condition will improve with additional running time.

The Van de Graaff and linear accelerator have been operated together for a total of about 30 hours, and results show that with comparable duty cycles the beam magnitudes obtained now are similar to those obtained before the changes were made. In one six hour period of operation only about 20 minutes beam time was lost due to oscillator trouble.

It has been suggested that immediate attempts be made to bunch the beam, so that further increase in the beam magnitude may be obtained.

Surveys are being made to estimate the amount of shielding required to protect personnel against the increased amount of radiation which is experienced when operating on longer pulse lengths, higher repetition rates, and more sustained operation.

5. Bevatron Development

W. M. Brobeck

During this period the majority of magnet steel was erected on the foundation and preparations were made for the start of coil winding. The coil end winding supports, which consist of large steel boxes, were all erected and the only steel erection remaining was the top yoke slabs which are not to be installed until after coil winding.

Installation of all the motor generator equipment was completed and most of the high current wiring was completed at the end of the period. Control wiring was the principal work remaining. At the end of the period the leads from the generator room to the magnet were being installed.

The magnet cooling fans have been installed and were tested during January. The air filter bank drawings have been completed but installation has not been started.

The tank and liner of the linear accelerator have been received but no assembly work is being done at the present time.

The test section of the vacuum envelope has been worked on during the period and is now almost ready for pumping down with the test pole assemblies in place. Progress has been slow because of difficulties in getting satisfactorily tight vacuum joints with the rubber gaskets. Design shortcomings and inaccuracies in machine work and gasket dimensions are responsible for this problem. No fundamental difficulties have occurred but progress has been slow due to low priority.

Only three or four engineers and draftsmen have been available for mechanical work on the Bevatron and consequently very little design work has been carried on during the period. Higher priority demands continue to interfere with future progress on the Bevatron engineering work. At the present time sufficient drawings exist for completion of the coil winding and for procurement of the magnet poles and some of the vacuum envelope parts.